THE ASTROPHYSICAL JOURNAL SUPPLEMENT SERIES, 128:371–385, 2000 May

SUBMILLIMETER-WAVE MEASUREMENTS AND ANALYSIS OF THE GROUND AND $\nu_2 = 1$ STATES OF WATER

PIN CHEN
Time and Frequency Division, National Institute of Standards and Technology, Mail Stop 847.10, 325 Broadway, Boulder, CO 80303
J. C. PEARSON AND HERBERT M. PICKETT
Jet Propulsion Laboratory, California Institute of Technology, Mail Stop 183-301, 4800 Oak Grove Drive, Pasadena, CA 91109
AND
SHUJI MATSUURA AND GEOFFREY A. BLAKE
Division of Geological and Planetary Sciences, California Institute of Technology, Mail Stop 150-21, Pasadena, CA 91125
Received 1999 July 15; accepted 1999 November 24

ABSTRACT

In order to facilitate further studies of water in the interstellar medium, the envelopes of late-type stars, jets, and shocked regions, the frequencies of 17 newly measured $H_2{}^{16}O$ transitions between 0.841 and 1.575 THz are reported. A complete update of the available water line frequencies and a detailed calculation of unmeasured rotational transitions and transition intensities as a function of temperature are presented for the ground and $\nu_2 = 1$ state levels below 3000 cm^{-1} of excitation energy. The new terahertz transitions were measured with a recently developed laser difference frequency spectrometer. Six of these transitions arise from the $\nu_2 = 1$ state, and the other 11 are in the ground state; all have lower state energies from 700 to 1750 cm^{-1} and should be accessible to Stratospheric Observatory For Infrared Astronomy (SOFIA) through the atmosphere. The transitions near 0.850 THz are accessible from the ground with existing receivers. Observations of the newly measured $\nu_2 = 1$ state transitions, which include the $1_{1,1}$–$0_{0,0}$ fundamental at 1.2057 THz and five other very low J transitions, should provide valuable insights into role played by the $\nu_2 = 1$ state in the cooling dynamics of jets, shocks, masers, and strongly infrared-pumped regions. The line list is presented to assist in the planning of observational campaigns with the *Far-Infrared Space Telescope* (FIRST) and other proposed space missions with which a full suite of water observations can be carried out.

Subject heading: infrared: ISM: lines and bands — ISM: molecules — methods: laboratory — molecular data

1. INTRODUCTION

Among the over 100 molecules now detected in the interstellar medium, water retains a special significance. Its strong dipole moment allows water vapor to contribute substantially to the cooling of interstellar gas over an extraordinary span of densities and temperatures, while its hydrogen bonding capabilities give it "universal solvent" properties, allowing it to exist in a liquid or solid state over a wide range of physical conditions. Thus, from a dynamical point of view, it plays a critical role in the chemical and physical evolution of galaxies, from young stars in dense molecular clouds to late-type stars or brown dwarfs. For a compositional point of view, water ice is the dominant component of volatile grain mantles in dense molecular clouds as well as planetesimals in the outer regions of the solar system. The so-called habitable zone, where existence of life as we know it is possible, is restricted to regions around stars in which terrestrial planets can maintain liquid water on their surfaces over geological timescales (Kasting, Whitmire, & Reynolds 1993). Because of such ubiquitous importance, the observation and characterization of water spectra have been intensely pursued in the astrophysical community, despite severe difficulties.

Observation of extraterrestrial water vapor has always posed a major experimental challenge because of its abundance in the atmosphere. Indeed, water vapor gives rise to most of the tropospheric atmospheric opacity from the millimeter-wave to far-infrared spectral region, and the need for low concentrations of atmospheric water is the primary selection criterion for the Atacama Large Millimeter Array (ALMA) and South Pole submillimeter sites (Radford & Holdaway 1998; Matsuo, Sakamoto, & Matushita 1998). Despite the low precipitable water columns at these sites, there are still large regions of completely inaccessible frequencies because of atmospheric absorption. For observations from the Stratospheric Observatory For Infrared Astronomy (SOFIA), the problem is less severe because of the increased altitude; however, direct studies of the strongest transitions are still precluded by the atmosphere. This problem is particularly acute for the low-lying ground-state transitions now known to dominate interstellar spectra.

In spite of the observational difficulties, a number of water transitions, both from the parent isotopomer and from isotopically substituted species such as $H_2{}^{18}O$ and HDO, have been observed from the ground and from the Kuiper Airborne Observatory (KAO). More recently, a large number of water transitions have been observed both in emission and absorption by spectrometers on board the *Infrared Space Observatory* (*ISO*; e.g., Neufeld et al. 1996; Liu et al. 1996). Two small observatories, NASA's *Submillimeter Wave Astronomy Satellite* (*SWAS*) and the Swedish Space Corporation's *Odin*, are beginning service with the primary mission goal of each being observations of the 557 GHz water fundamental (Melnick 1993; Melnick et al. 1996). On longer timescales, the *Far-Infrared Space Telescope* (*FIRST*) mission offers the potential for detailed studies of large numbers of water lines, including the majority of those presented here, free of the usual atmospheric restrictions. The recently launched and future observatories are anticipated to dramatically increase our understanding of the chemical composition, temperature, density, and cooling of the interstellar medium—provided that sufficiently accurate spectral information is available, either through theoretical predictions or fitting of experimental data, to enable analysis of observational data.

Prediction of water transitions with the kind of accuracy required for heterodyne observations remains an elusive goal. A number of authors have attempted a wide variety of analysis techniques with limited success. Unfortunately, where extrapolation of previously reported microwave data to higher J and K_a values is required, none of these methods have enabled microwave accuracy predictions. The current state of the art in the calculation of water frequencies is to use a potential energy surface based on ab initio calculations (Partridge & Schwenke 1997). Several different methods of generating ab initio line lists have been developed (Viti, Tennyson, & Polyansky 1997), and they have proven useful in assignment of the sunspot spectrum (Tennyson & Polyansky 1998; Polyansky et al. 1997a, 1997b). Under favorable conditions, the ab initio accuracy appears to be better than 0.01 cm^{-1}. This translates to errors of several hundred megahertz in the pure rotational line frequencies, which is insufficient for heterodyne astronomy requirements. However, there is considerable hope that additional high-resolution data, especially in the $v_2 = 1$ state, will eventually facilitate the accurate prediction of high J and K_a transitions at submillimeter frequencies. For the present time, it is still necessary to utilize fits to observed data for an accurate determination of the water vapor pure rotational spectrum.

Two distinct methods for fitting experimental water spectra have been proposed and demonstrated in the literature: (1) effective approaches to the rotational Hamiltonian, such as Padé series (Burenin et al. 1983; Burenin & Tyuterev 1984), Borel approximates (Polyansky 1985; Belov et al. 1987), and generating functions (Tyuterev 1992; Starikov, Tashkun, & Tyuterev 1992; Mikhailenko et al. 1997); and (2) a potential function that describes one or more vibrational degrees of freedom (usually the bend) is combined with an effective Hamiltonian that addresses the remaining degrees of freedom (Jensen 1989; Coudert 1992, 1994, 1997; Lanquetin, Coudert, & Camy-Peyret 1999). The best results will most likely emerge from the application of the second method using a version of the Partridge & Schwenke (1997) potential surface, empirically modified to reproduce the highest observed levels (e.g., Csaszar et al. 1998), and an effective Hamiltonian fit to the experimental data to secure the extra precision needed. The largest of these calculations have managed to reproduce the observed data to close to experimental accuracy, but they have not yet managed to achieve the accuracy needed for predictions of unobserved higher J and K_a transitions to heterodyne resolution (Coudert 1997). Some of the disparity is clearly due to the relatively small number of very high precision terahertz measurements in these previous works, especially in the $v_2 = 1$ state. Over the last few years a number of high-resolution far-infrared and infrared studies have been carried out, greatly improving the quality of the available water line data. In this paper the ground and $v_2 = 1$ state water spectra have been reanalyzed with a non–power series effective Hamiltonian. This approach has reproduced the data to within a factor of 2 of the experimental precision and pointed out a number of potential problems with the existing data set.

The other difficult problem in water spectroscopy is the accurate prediction of relative and absolute line intensities. The current wisdom is to use a power series expansion of the dipole moment tensor (Suhm & Watts 1991; Shostak, Ebenstein, & Muenter 1991; Shostak & Muenter 1991; Kjaergaard et al. 1994; Kjaergaard & Henry 1994; Mengel & Jensen 1995; Coudert 1997; Toth 1998). The most recent dipole expansions are in good agreement with the observed data for $J < 15$. However, the dipole expansion has yet to be applied to highly excited levels and is therefore likely to suffer from the same problems as the energy level calculations. As a result, little is known about how well these dipole expansions will predict intensities at larger rotational quantum numbers. Calculation of the intensities for the low-lying rotational transitions in the microwave region should be good to better than 5% with the two most recent dipole expansions. The greatest deviations from the predicted intensities are expected in the higher J transitions with $\Delta K_a > 3$. In the intensity calculations presented here, the measured dipole moment parameters of Shostak et al. (1991) and Shostak & Muenter (1991) have been used along with the planarity conditions as described by Watson (1971) in a computational method developed by Camy-Peyret et al. (1985).

The precision measurements of additional $H_2{}^{16}O$ transitions should facilitate their astronomical observation in addition to supporting efforts in developing better molecular models for the calculation of the energy levels and transition intensities. The measurements reported herein are among the first acquired with a new spectrometer system that uses optical-heterodyne conversion to generate terahertz radiation. The outstanding tuning capability of this spectrometer should facilitate the precision measurement of a variety of species in the 0.3–3.0 THz region in support of *FIRST* and SOFIA. The transition list reported by Pearson et al. (1991) is also updated to include the large number of high-accuracy measurements made over the last few years. The calculations presented represent the state of the art, and they should be sufficient for all far-infrared astronomical observations except those of the hottest and most highly shocked regions and prove useful in planning the terahertz heterodyne receiver science programs for *FIRST* and SOFIA.

2. EXPERIMENTAL

The experimental measurements were carried out with a three-diode laser difference-frequency spectrometer, an outline of which is presented in Figure 1. Laser 1 is locked, using a Pound-Drever-Hall approach (Pound 1946; Drever et al. 1983), to a temperature stabilized ultralow expansion (ULE) Fabry-Perot etalon. Laser 2 is Pound-Drever-Hall locked to the same etalon a large integer number of free spectral ranges away, and laser 3 is offset locked to laser 2. This offset frequency is controlled by a tunable 2–6 GHz microwave synthesizer. Beating simultaneously amplified signals from lasers 1 and 3 in a low-temperature–grown GaAs photomixer coupled to a planar submillimeter antenna (Verghese, McIntosh, & Brown 1997) generates the terahertz difference frequency. The free spectral range of the etalon was calibrated to 5 parts in 10^8 by measuring all CO pure rotational lines from 230 to 1611 GHz. A detailed

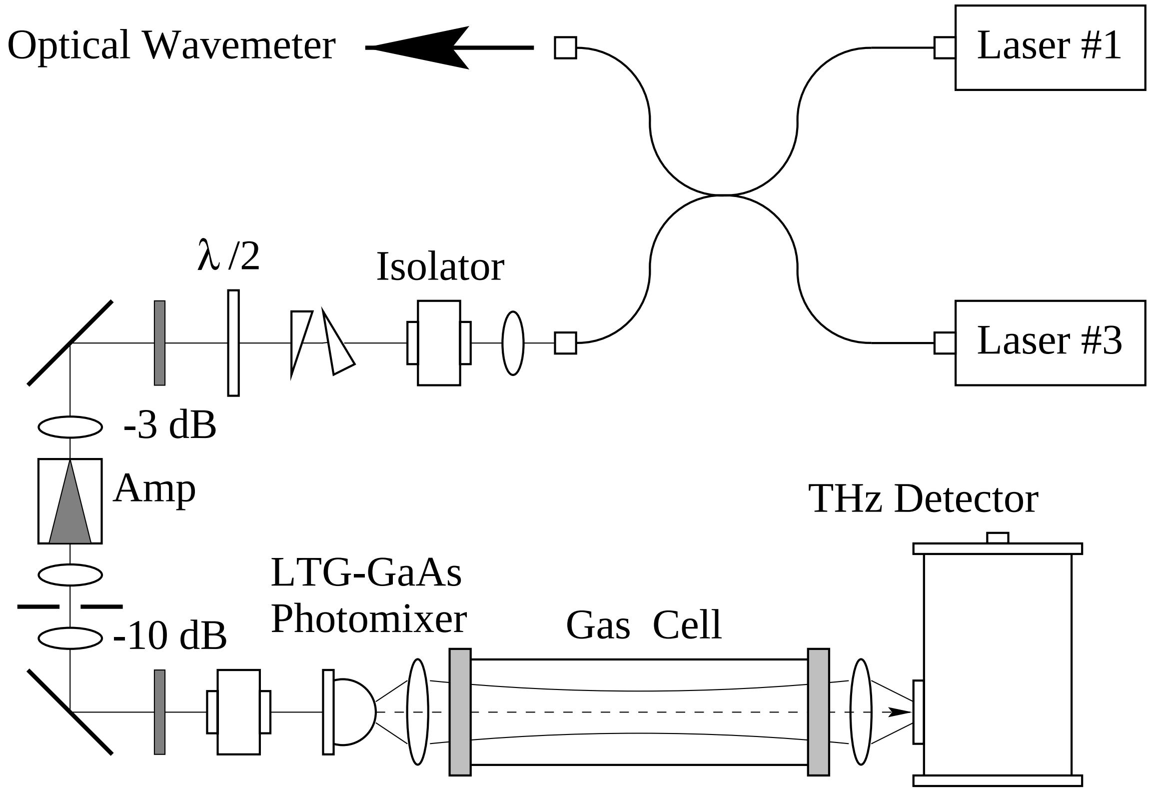

FIG. 1.—Schematic outline of the LTG-GaAs terahertz photomixer spectrometer. In this three-laser system, lasers 1 and 2 are locked to different longitudinal modes of a single ultralow thermal expansion coefficient reference cavity and laser 3 is phase locked to laser 2 with a tunable microwave source. Lasers 1 and 3 are used to form the tunable terahertz beat note.

description of this laser system and the calibration method can be found elsewhere (Matsuura et al. 2000). The measurement accuracy is currently limited by the uncertainty in the free spectral range, a small residual in the lock loops, and the accuracy of determining the center of the transition. The line width of the spectrometer is $\lesssim 1$ MHz (the terahertz frequency stability is considerably better), enabling Doppler-limited resolution to be obtained. As a result, the expected measurement accuracy is calculated to be of order 250 kHz for a 1 σ measurement. The $4_{2,\,2}$–$3_{3,\,1}$ ground state transition was remeasured as a verification of the spectrometer calibration. Our observed value of 916171.270 MHz agrees within the expected 250 kHz experimental error with both the 916171.582 (150) harmonic generation value reported by Helminger, Messer, & De Lucia (1983) and the 916171.405 (13) laser sideband value reported by Matsushima et al. (1995).

Initial predictions were made from energy levels calculated by Toth (1998) and from previous uncalibrated backward wave oscillator measurements (S. P. Belov 1996, private communication). The water sample was reagent grade and required no further processing. Measurements were made in a single pass 1.6 m long cell under slow continuous flow conditions at pressures of approximately 100 mtorr. A 1.8 K composite-silicon bolometer was used to detect the tunable terahertz radiation. The source was chopped at 100 Hz, and second-harmonic lock-in detection was used to record the line profiles. Forward and backward scans were averaged to eliminate the lock-in time constant drift, while the line centers were determined by either fitting a parabola to the peak of the observed transition or by taking the midpoint between the half-intensity frequencies. Signal-to-noise ratios for the observed lines ranged from 10 to $\gtrsim 500$. Several measurements of each line were made for consistency.

All the measured transitions fell within the experimental errors expected from the combination differences derived by Toth (1998). The agreement with the uncalibrated measurements by S. P. Belov (1996, private communication) is better than 1 MHz in all cases, suggesting that all of these uncalibrated measurements are accurate to this level. Table 1 presents the results of this study along with the expected positions from Toth (1998) and the uncalibrated measurements by S. P. Belov (1996, private communication). Clearly, all the reported transitions agree extremely well with the energy levels calculated by Toth (1998). This was expected since a series of combination difference calculations with our measurements and those by Matsushima et al. (1995) used in the Toth (1998) compilation closed to within experimental accuracy. Table 2 is a set of measurements by Pearson (1995) compared to the energy levels from Toth (1998) for the $v_2 = 1$ state and from Toth (1999) for the $v_2 = 2$ or (020), $v_1 = 1$ or (100) and $v_3 = 1$ or (001) states. Once again, all the measurements—with the exception of the 14 MHz deviation of the (020) $4_{2,\,2}$–$3_{3,\,1}$ transition—agree to within the experimental uncertainty. The reason for the large deviation of the $4_{2,\,2}$–$3_{3,\,1}$ transition is unclear and a cause for some concern. The 17 transitions measured as a part of this work, the two reported by S. P. Belov (1996, private communication), and the nine by Pearson (1995) have not appeared in the widely published literature. Table 3 presents a list of all the reported microwave accuracy measurements for $H_2{}^{16}O$ below 4 THz and also includes the observed minus calculated fre-

TABLE 1

WATER TRANSITIONS MEASURED WITH THE TERAHERTZ PHOTOMIXER SPECTROMETER

Transition $J_{K''_a,K''_c''} \rightarrow J_{K'_a,K'_c'}(V_1\ V_2\ V_3)$	Observed Frequency (MHz)	Toth 1998 (MHz)	Belov 1996 (priv. comm.) (MHz)
$10_{5,6} \rightarrow 11_{2,9}$ (000)	841051.162 (250)	841050.35 (1.50)	841050.56 (1.00)
$10_{8,3} \rightarrow 9_{9,0}$ (000)	...	863842.67 (2.70)	863838.93 (1.00)
$9_{2,8} \rightarrow 8_{3,5}$ (000)	906206.118 (250)	906205.78 (0.39)	...
$7_{2,5} \rightarrow 8_{1,8}$ (000)	1146621.161 (250)	1146621.04 (0.39)	...
$8_{5,4} \rightarrow 7_{6,1}$ (000)	1168358.526 (250)	1168358.57 (0.48)	...
$7_{4,4} \rightarrow 6_{5,1}$ (000)	1172525.835 (250)	1172525.90 (0.48)	...
$8_{5,3} \rightarrow 7_{6,2}$ (000)	1190828.878 (250)	1190828.80 (0.48)	...
$9_{6,4} \rightarrow 8_{7,1}$ (000)	1215801.676 (250)	1215801.87 (0.84)	...
$9_{6,3} \rightarrow 8_{7,2}$ (000)	1219943.736 (250)	1219943.68 (0.90)	...
$8_{4,5} \rightarrow 9_{1,8}$ (000)	1307963.124 (250)	1307963.17 (0.48)	...
$7_{4,4} \rightarrow 8_{1,7}$ (000)	1344676.488 (250)	1344676.29 (0.48)	...
$6_{4,3} \rightarrow 7_{1,6}$ (000)	1574232.073 (250)	1574232.14 (0.39)	...
$2_{1,1} \rightarrow 2_{0,2}$ (010)	859965.649 (250)	859966.36 (0.90)	...
$2_{0,2} \rightarrow 1_{1,1}$ (010)	899302.171 (250)	899301.23 (1.80)	899301.92 (1.00)
$3_{1,2} \rightarrow 2_{2,1}$ (010)	902609.436 (250)	902610.64 (2.70)	902609.31 (1.00)
$6_{2,5} \rightarrow 5_{3,2}$ (010)	...	923113.74 (1.80)	923113.19 (1.00)
$1_{1,1} \rightarrow 0_{0,0}$ (010)	1205788.640 (250)	1205788.95 (2.70)	...
$3_{1,2} \rightarrow 3_{0,3}$ (010)	1214662.064 (250)	1214663.11 (2.40)	...
$2_{2,0} \rightarrow 2_{1,1}$ (010)	1494057.154 (250)	1494057.39 (0.60)	...

quency differences and the lower state energy of the fit. The lower state energy calculated by Toth (1998) is given as well.

3. ANALYSIS

The experimental data used in the analysis included the following.

1. The microwave transitions reported in Table 3. These cover a range of J and K_a values to 17 and 9, respectively. The measurements by Matsushima et al. (1995) were assumed to have an experimental accuracy of 150 kHz. This was derived from a series of arithmetic calculation of residuals around closed loops of four transitions and is consistent with 5% of the FWHM of a water line profile at these frequencies.
2. The term values listed by Toth (1998) and Polyansky et al. (1997b) through $J = 19$ and 18 including all K_a values in the ground and $v_2 = 1$ states, respectively.
3. Infrared rotational transitions, including transitions covering J and K_a values to 21 and 15, respectively (Kauppinen, Karkkainen, & Kyro 1978; Johns 1985; Paso & Horneman 1995; R. A. Toth 1999, private communication).
4. Infrared v_2 band transitions measured by R. A. Toth (1999, private communication), with J and K_a values to 21 and 13, respectively.

TABLE 2

ADDITIONAL WATER TERAHERTZ MEASUREMENTS FROM PEARSON 1995

Transition $J_{K''_a,K''_c''} \rightarrow J_{K'_a,K'_c'}(V_1\ V_2\ V_3)$	Observed Frequency (MHz)	Toth 1998 (MHz)
$8_{8,1} \rightarrow 9_{7,2}$ (010)	129811.529 (100)	129812.23 (2.70)
$8_{8,0} \rightarrow 9_{7,3}$ (010)	129889.509 (100)	129889.28 (3.00)
$4_{2,2} \rightarrow 3_{3,1}$ (020)	137048.521 (100)	137062.41 (2.70)
$6_{3,3} \rightarrow 5_{4,2}$ (020)	147521.501 (100)	147521.57 (2.40)
$3_{1,3} \rightarrow 2_{2,0}$ (020)	516229.985 (150)	516230.02 (3.00)
$6_{4,3} \rightarrow 5_{5,0}$ (100)	376549.519 (150)	376549.52 (1.80)
$5_{3,3} \rightarrow 4_{4,0}$ (100)	464345.834 (150)	464345.84 (3.60)
$3_{1,3} \rightarrow 2_{2,0}$ (001)	254039.880 (150)	254039.33 (1.50)
$4_{1,4} \rightarrow 3_{2,1}$ (001)	430012.786 (150)	430012.11 (1.80)

In the event of repeated measurements, the value used in the fit was the microwave frequency or the most recent infrared measurement. The model used was a non–power series effective Hamiltonian related to both the Padé Series and the generating functions discussed in the introduction (§ 1). The details of the calculation and the model will be presented in an appropriate forum elsewhere (Pearson et al. 2000, in preparation). The reduced rms of the fit [reduced rms = absolute rms (MHz)/experimental error (MHz)] was 1.98 if all the data were forced into the fit and 1.61 if the fit were allowed to reject 13 of 3992 lines and energy levels. Reduced rms values of 1.78 and 1.41 were achieved with a slightly reduced data set, with the same exact same 13 lines being rejected in the reduced analysis. It is interesting to note that the majority of the rejected transitions (a total of eight) involved the $15_{6,10}$ level of the $v_2 = 1$ state and that the deviations were all of the same direction and magnitude to much better than the experimental accuracy, suggesting either a fitting artifact or a local perturbation. Because of the form of these deviations, the results presented here are from a fit in which all the transitions were forced into the calculation.

An analysis of the fit residuals shows that the measured transitions fit to nearly the experimental error and that much of the observed error is in energy levels derived by combination difference. This is especially true at the K_a values above those of the measured lines (e.g., $K_a > 16$). These energy levels were determined entirely by series of R ($\Delta J = -1$, $\Delta K_a = -1$) branch transitions and have uncertainties given by the cumulative measurement error going back to the first quantum level at which multiple combinations are possible. Lanquetin et al. (1999) has recently addressed the high-K_a data in detail. For K_a levels where there are combination differences (up to $K_a = 12$) to verify the reported experimental uncertainty, this calculation reproduces those levels to better than the reduced rms except in a few (13) isolated cases.

The intensity calculations used a Watson A-like constant set and a fixed S-like d_2 constant determined from the planarity conditions. The fixed d_2 constant can be removed,

TABLE 3

THE MICROWAVE AND TERAHERTZ DATA SET USED IN THE WATER SPECTRUM FIT

$J''_{K''_a K''_c} V''_2 \rightarrow J'_{K'_a K'_c} V'_2$	Frequency (MHz)	Observed Minus Computed (MHz)	Uncertainty (kHz)	Reference
$4_{2,2}\,1 \rightarrow 5_{1,5}\,1$..........	2159.980	−0.059	300	1
$4_{2,3}\,1 \rightarrow 3_{3,0}\,1$..........	12008.800	0.002	30	1
$6_{1,6}\,0 \rightarrow 5_{2,3}\,0$..........	22235.080	−0.037	20	1
$5_{3,2}\,1 \rightarrow 4_{4,1}\,1$..........	26834.270	0.029	30	1
$4_{1,4}\,1 \rightarrow 3_{2,1}\,1$..........	67803.960	−0.030	40	1
$4_{4,0}\,1 \rightarrow 5_{3,3}\,1$..........	96261.160	0.309	100	1
$2_{2,0}\,1 \rightarrow 3_{1,3}\,1$..........	119995.940	−0.195	100	1
$8_{8,1}\,1 \rightarrow 9_{7,2}\,1$..........	129811.529	0.157	150	2
$8_{8,0}\,1 \rightarrow 9_{7,3}\,1$..........	129889.509	−0.010	150	2
$14_{6,9}\,0 \rightarrow 15_{3,12}\,0$......	139614.293	1.320	150	1
$15_{6,10}\,0 \rightarrow 16_{3,13}\,0$.....	177317.068	−0.947	150	1
$3_{1,3}\,0 \rightarrow 2_{2,0}\,0$..........	183310.117	0.087	50	1
$5_{5,1}\,1 \rightarrow 6_{4,2}\,1$..........	209118.370	−0.012	150	1
$5_{5,0}\,1 \rightarrow 6_{4,3}\,1$..........	232686.700	0.145	150	1
$14_{4,10}\,0 \rightarrow 15_{3,13}\,0$.....	247440.096	−0.051	150	1
$13_{6,8}\,0 \rightarrow 14_{3,11}\,0$......	259951.444	−1.169	150	1
$7_{7,1}\,1 \rightarrow 8_{6,2}\,1$..........	262897.748	0.120	150	1
$7_{7,0}\,1 \rightarrow 8_{6,3}\,1$..........	263451.357	−0.169	150	1
$6_{6,1}\,1 \rightarrow 7_{5,2}\,1$..........	293664.442	0.044	150	1
$6_{6,0}\,1 \rightarrow 7_{5,3}\,1$..........	297439.107	−0.307	150	1
$10_{2,9}\,0 \rightarrow 9_{3,6}\,0$	321225.640	−0.016	50	1
$14_{3,12}\,1 \rightarrow 13_{4,9}\,1$......	323554.019	0.293	150	1
$5_{1,5}\,0 \rightarrow 4_{2,2}\,0$..........	325152.919	−0.016	50	1
$5_{2,3}\,1 \rightarrow 6_{1,6}\,1$..........	336227.620	−0.311	150	1
$16_{6,11}\,0 \rightarrow 17_{3,14}\,0$.....	339043.996	0.320	150	1
$17_{4,13}\,0 \rightarrow 16_{7,10}\,0$.....	354808.877	0.051	150	1
$4_{1,4}\,0 \rightarrow 3_{2,1}\,0$..........	380197.372	0.006	50	1
$10_{3,7}\,0 \rightarrow 11_{2,10}\,0$......	390134.508	−0.133	50	1
$8_{5,4}\,1 \rightarrow 7_{6,1}\,1$..........	425689.190	−0.101	150	1
$7_{5,3}\,0 \rightarrow 6_{6,0}\,0$..........	437346.667	0.016	50	1
$9_{6,4}\,1 \rightarrow 8_{7,1}\,1$..........	438724.178	1.149	150	1
$6_{4,3}\,0 \rightarrow 5_{5,0}\,0$..........	439150.812	−0.059	50	1
$8_{5,3}\,1 \rightarrow 7_{6,2}\,1$..........	440736.910	−0.796	150	1
$9_{6,3}\,1 \rightarrow 8_{7,2}\,1$..........	441238.866	−0.406	150	1
$7_{5,2}\,0 \rightarrow 6_{6,1}\,0$..........	443018.295	−0.017	50	1
$4_{2,3}\,0 \rightarrow 3_{3,0}\,0$..........	448001.075	−0.059	50	1
$4_{2,2}\,1 \rightarrow 3_{3,1}\,1$..........	463170.460	−0.243	250	1
$6_{4,2}\,0 \rightarrow 5_{5,1}\,0$..........	470888.947	−0.056	50	1
$5_{3,3}\,0 \rightarrow 4_{4,0}\,0$..........	474689.127	−0.130	50	1
$6_{2,4}\,0 \rightarrow 7_{1,7}\,0$..........	488491.133	0.061	50	1
$7_{4,4}\,1 \rightarrow 6_{5,1}\,1$..........	498502.590	0.241	150	1
$8_{6,3}\,0 \rightarrow 7_{7,0}\,0$..........	503568.532	−0.305	100	1
$8_{6,2}\,0 \rightarrow 7_{7,1}\,0$..........	504482.692	−0.307	100	1
$14_{3,12}\,0 \rightarrow 13_{4,9}\,0$......	530342.834	0.083	150	1
$5_{2,4}\,1 \rightarrow 4_{3,1}\,1$..........	546690.600	−0.098	150	1
$10_{7,4}\,1 \rightarrow 9_{8,1}\,1$	548474.403	−0.524	150	1
$1_{1,0}\,0 \rightarrow 1_{0,1}\,0$..........	556936.002	0.014	50	1
$12_{6,7}\,0 \rightarrow 13_{3,10}\,0$......	571913.392	−0.729	150	1
$7_{4,3}\,1 \rightarrow 6_{5,2}\,1$..........	578057.486	0.206	150	1
$9_{2,8}\,1 \rightarrow 8_{3,5}\,1$..........	593708.497	−0.192	150	1
$6_{3,4}\,1 \rightarrow 5_{4,1}\,1$..........	595079.800	−0.158	150	1
$5_{3,2}\,0 \rightarrow 4_{4,1}\,0$..........	620700.807	−0.308	100	1
$9_{7,3}\,0 \rightarrow 8_{8,0}\,0$..........	645766.010	−0.044	100	1
$9_{7,2}\,0 \rightarrow 8_{8,1}\,0$..........	645905.620	0.056	100	1
$1_{1,0}\,1 \rightarrow 1_{0,1}\,1$..........	658006.550	0.075	100	1
$2_{1,1}\,0 \rightarrow 2_{0,2}\,0$..........	752033.227	0.095	100	1
$10_{5,6}\,0 \rightarrow 11_{2,9}\,0$	841051.162	0.689	250	3
$2_{1,1}\,1 \rightarrow 2_{0,2}\,1$..........	859965.649	0.228	250	3
$10_{8,3}\,0 \rightarrow 9_{9,0}\,0$	863838.930	1.908	1000	4
$2_{0,2}\,1 \rightarrow 1_{1,1}\,1$..........	899302.171	0.188	250	3
$3_{1,2}\,1 \rightarrow 2_{2,1}\,1$..........	902609.436	0.078	250	3
$9_{2,8}\,0 \rightarrow 8_{3,5}\,0$..........	906206.118	0.179	250	3
$4_{2,2}\,0 \rightarrow 3_{3,1}\,0$..........	916171.582	0.073	100	1

TABLE 3—*Continued*

$J''_{K''_a K''_c} V''_2 \rightarrow J'_{K'_a K'_c} V'_2$	Frequency (MHz)	Observed Minus Computed (MHz)	Uncertainty (kHz)	Reference
$6_{2,5}\,1 \rightarrow 5_{3,2}\;1$	923113.190	−0.374	1000	4
$5_{2,4}\,0 \rightarrow 4_{3,1}\;0$	970315.022	−0.075	100	1
$3_{1,2}\,0 \rightarrow 3_{0,3}\;0$	1097364.791	−0.114	150	5
$1_{1,1}\,0 \rightarrow 0_{0,0}\;0$	1113342.964	0.047	150	5
$7_{2,5}\,0 \rightarrow 8_{1,8}\;0$	1146621.161	−0.161	250	3
$3_{1,2}\,0 \rightarrow 2_{2,1}\;0$	1153126.822	0.146	150	5
$6_{3,4}\,0 \rightarrow 5_{4,1}\;0$	1158323.743	−0.149	150	5
$3_{2,1}\,0 \rightarrow 3_{1,2}\;0$	1162911.593	−0.107	150	5
$8_{5,4}\,0 \rightarrow 7_{6,1}\;0$	1168358.526	0.009	250	3
$7_{4,4}\,0 \rightarrow 6_{5,1}\;0$	1172525.835	−0.024	250	3
$8_{5,3}\,0 \rightarrow 7_{6,2}\;0$	1190828.878	−0.014	250	3
$1_{1,1}\,1 \rightarrow 0_{0,0}\;1$	1205788.640	−0.663	250	3
$4_{2,2}\,0 \rightarrow 4_{1,3}\;0$	1207638.714	0.002	150	5
$3_{1,2}\,1 \rightarrow 3_{0,3}\;1$	1214662.064	0.295	250	3
$9_{6,4}\,0 \rightarrow 8_{7,1}\;0$	1215801.676	−0.060	250	3
$9_{6,3}\,0 \rightarrow 8_{7,2}\;0$	1219943.736	−0.638	250	3
$2_{2,0}\,0 \rightarrow 2_{1,1}\;0$	1228788.772	−0.068	150	5
$7_{4,3}\,0 \rightarrow 6_{5,2}\;0$	1278265.946	0.023	150	5
$8_{2,7}\,0 \rightarrow 7_{3,4}\;0$	1296411.033	−0.016	150	5
$8_{4,5}\,0 \rightarrow 9_{1,8}\;0$	1307963.124	−0.163	250	3
$6_{2,5}\,0 \rightarrow 5_{3,2}\;0$	1322064.803	0.020	150	5
$7_{4,4}\,0 \rightarrow 8_{1,7}\;0$	1344676.488	0.312	250	3
$5_{2,3}\,0 \rightarrow 5_{1,4}\;0$	1410618.074	0.087	150	5
$7_{2,6}\,0 \rightarrow 6_{3,3}\;0$	1440781.544	−0.121	150	5
$2_{2,0}\,1 \rightarrow 2_{1,1}\;1$	1494057.154	−0.332	250	3
$6_{3,3}\,0 \rightarrow 5_{4,2}\;0$	1541966.785	−0.265	150	5
$6_{4,3}\,0 \rightarrow 7_{1,6}\;0$	1574232.073	0.006	250	3
$4_{1,3}\,0 \rightarrow 4_{0,4}\;0$	1602219.182	−0.160	150	5
$2_{2,1}\,0 \rightarrow 2_{1,2}\;0$	1661007.637	−0.125	150	5
$2_{1,2}\,0 \rightarrow 1_{0,1}\;0$	1669904.775	0.023	150	5
$4_{3,2}\,0 \rightarrow 5_{0,5}\;0$	1713882.973	0.021	150	5
$3_{0,3}\,0 \rightarrow 2_{1,2}\;0$	1716769.633	0.100	150	5
$6_{3,3}\,0 \rightarrow 6_{2,4}\;0$	1762042.791	0.132	150	5
$7_{3,5}\,0 \rightarrow 6_{4,2}\;0$	1766198.748	0.005	150	5
$6_{2,4}\,0 \rightarrow 6_{1,5}\;0$	1794788.953	0.030	150	5
$7_{3,4}\,0 \rightarrow 7_{2,5}\;0$	1797158.762	0.029	150	5
$5_{3,2}\,0 \rightarrow 5_{2,3}\;0$	1867748.594	0.127	150	5
$8_{4,5}\,0 \rightarrow 7_{5,2}\;0$	1884887.822	−0.091	150	5
$5_{2,3}\,0 \rightarrow 4_{3,2}\;0$	1918485.324	−0.117	150	5
$3_{2,2}\,0 \rightarrow 3_{1,3}\;0$	1919359.531	0.011	150	5
$8_{3,5}\,0 \rightarrow 8_{2,6}\;0$	2015982.828	−0.019	150	5
$4_{3,1}\,0 \rightarrow 4_{2,2}\;0$	2040476.810	0.051	150	5
$4_{1,3}\,0 \rightarrow 3_{2,2}\;0$	2074432.305	−0.076	150	5
$3_{1,3}\,0 \rightarrow 2_{0,2}\;0$	2164131.980	−0.021	150	5
$3_{3,0}\,0 \rightarrow 3_{2,1}\;0$	2196345.756	−0.034	150	5
$5_{1,4}\,0 \rightarrow 5_{0,5}\;0$	2221750.500	0.094	150	5
$8_{3,6}\,0 \rightarrow 7_{4,3}\;0$	2244810.924	−0.130	150	5
$4_{2,3}\,0 \rightarrow 4_{1,4}\;0$	2264149.650	0.092	150	5
$9_{4,5}\,0 \rightarrow 9_{3,6}\;0$	2317882.160	0.056	150	5
$7_{2,5}\,0 \rightarrow 7_{1,6}\;0$	2344250.335	−0.027	150	5
$10_{4,6}\,0 \rightarrow 10_{3,7}\;0$	2347482.172	0.133	150	5
$3_{3,1}\,0 \rightarrow 3_{2,2}\;0$	2365899.659	0.074	150	5
$4_{0,4}\,0 \rightarrow 3_{1,3}\;0$	2391572.628	0.068	150	5
$9_{3,6}\,0 \rightarrow 9_{2,7}\;0$	2428247.209	−0.115	150	5
$8_{4,4}\,0 \rightarrow 8_{3,5}\;0$	2446843.245	−0.122	150	5
$4_{3,2}\,0 \rightarrow 4_{2,3}\;0$	2462933.032	0.045	150	5
$9_{3,7}\,0 \rightarrow 8_{4,4}\;0$	2531917.811	0.097	150	5
$7_{3,4}\,0 \rightarrow 6_{4,3}\;0$	2567177.132	0.104	150	5
$11_{4,7}\,0 \rightarrow 11_{3,8}\;0$	2571762.630	0.113	150	5
$10_{3,8}\,0 \rightarrow 9_{4,5}\;0$	2575004.634	0.216	150	5
$5_{3,3}\,0 \rightarrow 5_{2,4}\;0$	2630959.520	0.146	150	5
$4_{1,4}\,0 \rightarrow 3_{0,3}\;0$	2640473.836	−0.135	150	5
$7_{4,3}\,0 \rightarrow 7_{3,4}\;0$	2664570.704	−0.080	150	5
$5_{2,4}\,0 \rightarrow 5_{1,5}\;0$	2685638.969	0.048	150	5

TABLE 3—*Continued*

$J''_{K''_a K''_c} V''_2 \rightarrow J'_{K'_a K'_c} V'_2$	Frequency (MHz)	Observed Minus Computed (MHz)	Uncertainty (kHz)	Reference
$2_{2,1}\,0 \rightarrow 1_{1,0}\,0$	2773976.588	0.062	150	5
$12_{5,7}\,0 \rightarrow 12_{4,8}\,0$	2848996.260	0.468	150	5
$6_{3,4}\,0 \rightarrow 6_{2,5}\,0$	2880025.369	0.075	150	5
$6_{1,5}\,0 \rightarrow 6_{0,6}\,0$	2884278.940	0.055	150	5
$6_{4,2}\,0 \rightarrow 6_{3,3}\,0$	2884941.052	0.012	150	5
$6_{2,4}\,0 \rightarrow 5_{3,3}\,0$	2962111.094	−0.098	150	5
$2_{2,0}\,0 \rightarrow 1_{1,1}\,0$	2968748.654	0.134	150	5
$5_{1,4}\,0 \rightarrow 4_{2,3}\,0$	2970800.244	−0.196	150	5
$11_{5,6}\,0 \rightarrow 11_{4,7}\,0$	2997539.160	0.364	150	5
$8_{2,6}\,0 \rightarrow 8_{1,7}\,0$	2998565.722	0.106	150	5
$10_{3,7}\,0 \rightarrow 10_{2,8}\,0$	3003347.566	−0.031	150	5
$5_{0,5}\,0 \rightarrow 4_{1,4}\,0$	3013199.566	−0.027	150	5
$5_{4,1}\,0 \rightarrow 5_{3,2}\,0$	3043766.149	−0.036	150	5
$10_{4,7}\,0 \rightarrow 9_{5,4}\,0$	3118998.512	−0.730	150	5
$4_{4,0}\,0 \rightarrow 4_{3,1}\,0$	3126585.070	−0.144	150	5
$5_{1,5}\,0 \rightarrow 4_{0,4}\,0$	3135010.951	−0.038	150	5
$9_{4,5}\,0 \rightarrow 8_{5,4}\,0$	3149876.898	−0.069	150	5
$4_{4,1}\,0 \rightarrow 4_{3,2}\,0$	3165532.734	−0.059	150	5
$6_{2,5}\,0 \rightarrow 6_{1,6}\,0$	3167578.237	0.103	150	5
$5_{4,2}\,0 \rightarrow 5_{3,3}\,0$	3182186.848	0.047	150	5
$7_{3,5}\,0 \rightarrow 7_{2,6}\,0$	3210358.196	0.078	150	5
$6_{4,3}\,0 \rightarrow 6_{3,4}\,0$	3230146.525	0.107	150	5
$10_{5,5}\,0 \rightarrow 10_{4,6}\,0$	3245323.573	0.269	150	5
$11_{5,7}\,0 \rightarrow 10_{6,4}\,0$	3307402.532	−0.528	150	5
$7_{4,4}\,0 \rightarrow 7_{3,5}\,0$	3329185.239	0.037	150	5
$3_{2,2}\,0 \rightarrow 2_{1,1}\,0$	3331458.376	−0.014	150	5
$8_{4,5}\,0 \rightarrow 8_{3,6}\,0$	3495358.110	−0.095	150	5
$9_{5,4}\,0 \rightarrow 9_{4,5}\,0$	3509431.278	−0.005	150	5
$7_{1,6}\,0 \rightarrow 7_{0,7}\,0$	3536666.807	0.096	150	5
$6_{0,6}\,0 \rightarrow 5_{1,5}\,0$	3599641.708	0.029	150	5
$8_{3,6}\,0 \rightarrow 8_{2,7}\,0$	3612970.623	−0.165	150	5
$6_{1,6}\,0 \rightarrow 5_{0,5}\,0$	3654603.282	−0.228	150	5
$8_{3,5}\,0 \rightarrow 7_{4,4}\,0$	3669872.251	−0.036	150	5
$11_{3,8}\,0 \rightarrow 11_{2,9}\,0$	3674226.995	−0.175	150	5
$9_{2,7}\,0 \rightarrow 9_{1,8}\,0$	3682708.105	0.046	150	5
$7_{2,6}\,0 \rightarrow 7_{1,7}\,0$	3691315.309	−0.088	150	5
$11_{5,6}\,0 \rightarrow 10_{6,5}\,0$	3718095.940	0.223	150	5
$8_{5,3}\,0 \rightarrow 8_{4,4}\,0$	3721502.796	0.058	150	5
$9_{4,6}\,0 \rightarrow 9_{3,7}\,0$	3737021.532	0.030	150	5
$6_{1,5}\,0 \rightarrow 5_{2,4}\,0$	3798281.638	−0.005	150	5
$4_{2,3}\,0 \rightarrow 3_{1,2}\,0$	3807258.412	−0.213	150	5
$7_{5,2}\,0 \rightarrow 7_{4,3}\,0$	3855281.595	0.250	150	5
$6_{5,1}\,0 \rightarrow 6_{4,2}\,0$	3922858.136	0.050	150	5
$8_{5,4}\,0 \rightarrow 8_{4,5}\,0$	3970997.405	0.173	150	5
$3_{2,1}\,0 \rightarrow 2_{1,2}\,0$	3977046.481	0.343	150	5
$7_{2,5}\,0 \rightarrow 6_{3,4}\,0$	4000164.750	0.037	150	5
$9_{5,5}\,0 \rightarrow 9_{4,6}\,0$	4020094.138	−0.019	150	5
$10_{4,7}\,0 \rightarrow 10_{3,8}\,0$	4053426.066	−0.042	150	5
$9_{3,7}\,0 \rightarrow 9_{2,8}\,0$	4072555.267	0.126	150	5
$10_{5,6}\,0 \rightarrow 10_{4,7}\,0$	4118633.703	−0.212	150	5
$8_{1,7}\,0 \rightarrow 8_{0,8}\,0$	4161918.741	0.011	150	5
$7_{0,7}\,0 \rightarrow 6_{1,6}\,0$	4166851.176	0.109	150	5
$7_{1,7}\,0 \rightarrow 6_{0,6}\,0$	4190576.643	−0.093	150	5
$5_{2,4}\,0 \rightarrow 4_{1,3}\,0$	4218430.618	0.050	150	5
$8_{2,7}\,0 \rightarrow 8_{1,8}\,0$	4240191.823	0.718	150	5
$11_{5,7}\,0 \rightarrow 11_{4,8}\,0$	4279695.925	0.241	150	5
$10_{2,8}\,0 \rightarrow 10_{1,9}\,0$	4345505.100	0.161	150	5
$11_{6,5}\,0 \rightarrow 11_{5,6}\,0$	4348518.162	−0.500	150	5
$12_{3,9}\,0 \rightarrow 12_{2,10}\,0$	4366791.768	−0.313	150	5
$11_{4,8}\,0 \rightarrow 11_{3,9}\,0$	4435759.411	0.550	150	5
$3_{3,0}\,0 \rightarrow 3_{0,3}\,0$	4456621.984	−0.411	150	5
$3_{3,1}\,0 \rightarrow 2_{2,0}\,0$	4468569.050	−0.084	150	5
$3_{3,0}\,0 \rightarrow 2_{2,1}\,0$	4512384.121	−0.045	150	5
$10_{6,4}\,0 \rightarrow 10_{5,5}\,0$	4519563.921	−0.217	150	5

TABLE 3—*Continued*

$J''_{K_a''K_c''}V_2'' \rightarrow J'_{K_a'K_c'}V_2'$	Frequency (MHz)	Observed Minus Computed (MHz)	Uncertainty (kHz)	Reference
$7_{1,6}\,0 \rightarrow 6_{2,5}\,0$	4535939.553	−0.092	150	5
$10_{3,8}\,0 \rightarrow 10_{2,9}\,0$	4571661.011	0.146	150	5
$6_{2,5}\,0 \rightarrow 5_{1,4}\,0$	4600431.452	0.214	150	5
$9_{6,3}\,0 \rightarrow 9_{5,4}\,0$	4619371.406	−0.203	150	5
$8_{6,2}\,0 \rightarrow 8_{5,3}\,0$	4668678.294	−0.098	150	5
$10_{6,5}\,0 \rightarrow 10_{5,6}\,0$	4684382.106	−0.187	150	5
$9_{6,4}\,0 \rightarrow 9_{5,5}\,0$	4684697.855	0.145	150	5
$7_{6,1}\,0 \rightarrow 7_{5,2}\,0$	4687526.543	−0.086	150	5
$6_{6,0}\,0 \rightarrow 6_{5,1}\,0$	4689524.212	−0.153	150	5
$8_{6,3}\,0 \rightarrow 8_{5,4}\,0$	4690093.784	−0.050	150	5
$6_{6,1}\,0 \rightarrow 6_{5,2}\,0$	4690528.924	−0.033	150	5
$7_{6,2}\,0 \rightarrow 7_{5,3}\,0$	4693044.499	0.156	150	5
$8_{0,8}\,0 \rightarrow 7_{1,7}\,0$	4724263.773	−0.037	150	5
$8_{1,8}\,0 \rightarrow 7_{0,7}\,0$	4734296.171	0.420	150	5
$9_{1,8}\,0 \rightarrow 9_{0,9}\,0$	4764038.870	−0.186	150	5
$9_{2,8}\,0 \rightarrow 9_{1,9}\,0$	4801938.995	0.088	150	5
$9_{3,6}\,0 \rightarrow 8_{4,5}\,0$	4802992.161	0.065	150	5
$4_{3,1}\,0 \rightarrow 4_{0,4}\,0$	4850334.680	−0.133	150	5
$12_{4,9}\,0 \rightarrow 12_{3,10}\,0$	4869963.371	−0.183	150	5

REFERENCES.—(1) Pearson et al. 1991; (2) Pearson 1995; (3) this work; (4) Belov 1996, private communication; (5) Matsushima et al. 1995.

however, and quality of the fit is largely unchanged. Higher order contributions to the dipole were calculated using the procedure presented by Camy-Peyret et al. (1985). The intensities generated by these calculations were compared to those found by Toth (1998) at 296 K and were found to be in reasonable agreement for all transitions changing K_a by 1 or 3. Since the dipole expansion used does not include the planarity conditions for the P^6 and higher order terms, transition intensities for $\Delta K_a > 3$ will not be correct. Large deviations do in fact exist between the measured intensities and the calculated values, but such transitions are not important in the terahertz region.

Table 4 contains a listing of all of the water rotational transitions below 4 THz and 3000 cm^{-1} of total energy. It includes the calculated frequency, the calculated uncertainty in the line position, the ${}^xS_{ba}\,\mu^2$ values, the lower and upper state energies state energies, and the factors $(e^{-E''/kT} - e^{-E'/kT})$ at 50, 200, 800, and 1500 K. The error in the calculation frequency assumes that the reduced rms of the fit is 1; since it is nearly 2, the error quoted is approximately 0.5 σ. The partition function determined as a function of temperature by a sum over all states up to $J = 23$ is listed in Table 5. It does not include contributions for higher J states or the next higher set of vibrational levels. At temperatures above 500 K, these levels will begin to contribute significantly, and by 1500 K they must be included if accurate values are to be determined. To first order, the partition function can be corrected by separating the vibrational part of the partition function and calculating a correction factor. A first-order correction for the vibrational states, (020), (100), (001), (030), (110) and (011), all of which have rotational levels below the energy considered in the rotational part of the calculation, is also given in Table 5. Multiplication of the rotational partition function given by the correction factor will give a better estimate of the true partition function at high temperatures, but it will not take care of contributions from higher rotational states. A full calculation, including the ν_2 band, will be placed in the JPL spectral line catalog on the World Wide Web.[1] A graphical summary of the local thermodynamic equilibrium (LTE) line intensities at various temperatures for a fixed column density is presented in Figure 2. By 1500 K the majority of the lines are within a factor of a few in intensity, and the strongest lines are from states that are relatively weak at room temperature and almost unpopulated at typical dense molecular cloud temperatures. It should also be noted that there is a 2 order of magnitude reduction in the intensity of the strongest line.

The LTE line intensities and other parameters can be calculated from the data given on *f* in Tables 4 and 5 using the following equations:

$$I_{ba}(T) = (8\pi^3/3hc)\nu^x_{ba}\,S_{ba}\,\mu^2[e^{-E''/kT} - e^{-E'/kT}]/Q_{\rm rs}\ , \quad (1)$$

$$I_{ba}(T) = I_{ba}(T_0)[Q_{\rm rs}(T_0)/Q_{\rm rs}(T)] \times [(e^{-E''/kT} - e^{-E'/kT})/(e^{-E''/kT_0} - e^{-E'/kT_0})]\ , \quad (2)$$

and

$$I_{ba}(T) = I_{ba}(T_0)(T_0/T)^{5/2}e^{-(1/T - 1/T_0)E''/k}\ . \quad (3)$$

In equation (1), ν_{ba} is the line frequency, ${}^xS_{ba}$ is the line strength including the degeneracy factors, μ is the dipole moment along the *b*-axis, E'' and E' are the lower and upper state energies, respectively, and $Q_{\rm rs}$ is the rotation-spin partition function.

The line frequency and LTE intensity data alone are, of course, insufficient to explain the excitation of water in the interstellar medium—especially the 1594 cm^{-1} $\nu_2 = 1$ state

[1] The JPL spectral line catalog is available on the World Wide Web at http://spec.jpl.nasa.gov.

TABLE 4

PREDICTED TERAHERTZ WATER TRANSITIONS AND INTENSITIES

Transition	ν_{ab} (MHz)	Uncertainty ($\frac{1}{2}$ σ)	E_l (cm^{-1})	$\mu^2 S$	I (50 K)	I (200 K)	I (800 K)	I (1500 K)
$4_{2,2}$–$5_{1,5}$ (010)	2160.039	0.061	1922.8290	0.3861	2.374 (−33)	5.093 (−10)	4.080 (−06)	1.093 (−05)
$9_{3,6}$–$10_{2,9}$ (010)	7257.123	0.154	2904.4283	1.3478	3.683 (−48)	1.466 (−12)	2.345 (−06)	1.432 (−05)
$4_{2,3}$–$3_{3,0}$ (010)	12008.798	0.029	1907.6157	1.3443	2.267 (−32)	3.155 (−09)	2.330 (−05)	6.164 (−05)
$6_{1,6}$–$5_{2,3}$ (000)	22235.117	0.010	446.5107	0.5975	2.787 (−09)	2.143 (−04)	5.971 (−04)	4.634 (−04)
$5_{3,2}$–$4_{4,1}$ (010)	26834.241	0.028	2129.5992	1.2204	1.711 (−35)	1.425 (−09)	3.492 (−05)	1.113 (−04)
$4_{1,4}$–$3_{2,1}$ (010)	67803.990	0.036	1819.3351	1.4393	2.965 (−30)	3.340 (−08)	1.540 (−04)	3.784 (−04)
$4_{4,0}$–$5_{3,3}$ (010)	96260.851	0.055	2126.4077	0.3994	6.605 (−35)	5.188 (−09)	1.257 (−04)	4.000 (−04)
$2_{2,0}$–$3_{1,3}$ (010)	119996.136	0.059	1739.4837	0.3630	8.993 (−29)	1.043 (−07)	3.141 (−04)	7.224 (−04)
$3_{1,3}$–$2_{2,0}$ (000)	183310.030	0.013	136.1639	0.3501	1.473 (−03)	1.616 (−02)	8.561 (−03)	5.132 (−03)
$5_{5,1}$–$6_{4,2}$ (010)	209118.382	0.068	2399.1654	0.3508	7.369 (−39)	1.563 (−09)	1.667 (−04)	6.677 (−04)
$5_{5,0}$–$6_{4,3}$ (010)	232686.556	0.072	2398.3815	1.0503	8.321 (−39)	1.744 (−09)	1.856 (−04)	7.433 (−04)
$14_{4,10}$–$15_{3,13}$ (000)	247440.147	0.130	2872.5805	0.4090	3.432 (−46)	6.109 (−11)	8.407 (−05)	5.014 (−04)
$13_{6,8}$–$14_{3,11}$ (000)	259952.613	0.092	2739.4285	0.4405	4.304 (−44)	1.670 (−10)	1.122 (−04)	5.984 (−04)
$6_{6,1}$–$7_{5,2}$ (010)	293664.398	0.080	2724.1671	0.9482	8.259 (−44)	2.097 (−10)	1.301 (−04)	6.856 (−04)
$6_{6,0}$–$7_{5,3}$ (010)	297439.414	0.080	2724.0414	0.3160	8.385 (−44)	2.125 (−10)	1.318 (−04)	6.945 (−04)
$10_{2,9}$–$9_{3,6}$ (000)	321225.656	0.025	1282.9191	0.9915	2.909 (−21)	7.279 (−06)	1.900 (−03)	2.987 (−03)
$5_{1,5}$–$4_{2,2}$ (000)	325152.935	0.011	315.7795	0.3150	3.769 (−06)	7.741 (−03)	1.095 (−02)	7.645 (−03)
$5_{2,3}$–$6_{1,6}$ (010)	336227.931	0.093	2042.7533	0.7731	4.075 (−33)	3.215 (−08)	5.068 (−04)	1.508 (−03)
$4_{1,4}$–$3_{2,1}$ (000)	380197.366	0.011	212.1564	1.2760	1.777 (−04)	1.895 (−02)	1.540 (−02)	9.865 (−03)
$10_{3,7}$–$11_{2,10}$ (000)	390134.641	0.041	1525.1360	0.2468	5.593 (−25)	1.535 (−06)	1.489 (−03)	2.873 (−03)
$8_{5,4}$–$7_{6,1}$ (010)	425689.291	0.080	2905.4335	2.4896	1.639 (−46)	8.124 (−11)	1.356 (−04)	8.335 (−04)
$7_{5,3}$–$6_{6,0}$ (000)	437346.651	0.017	1045.0583	0.3325	1.930 (−17)	5.411 (−05)	3.953 (−03)	5.100 (−03)
$6_{4,3}$–$5_{5,0}$ (000)	439150.871	0.016	742.0763	1.1077	1.047 (−12)	4.804 (−04)	6.845 (−03)	6.847 (−03)
$8_{5,3}$–$7_{6,2}$ (010)	440737.706	0.081	2905.4306	0.8307	1.683 (−46)	8.396 (−11)	1.403 (−04)	8.627 (−04)
$7_{5,2}$–$6_{6,1}$ (000)	443018.312	0.016	1045.0579	0.9980	1.949 (−17)	5.478 (−05)	4.004 (−03)	5.165 (−03)
$4_{2,3}$–$3_{3,0}$ (000)	448001.134	0.014	285.4186	1.3850	1.446 (−05)	1.308 (−02)	1.587 (−02)	1.082 (−02)
$4_{2,2}$–$3_{3,1}$ (010)	463170.703	0.082	1907.4514	0.5251	6.798 (−31)	1.155 (−07)	8.870 (−04)	2.361 (−03)
$6_{4,2}$–$5_{5,1}$ (000)	470889.003	0.016	742.0730	0.3704	1.103 (−12)	5.132 (−04)	7.333 (−03)	7.339 (−03)
$5_{3,3}$–$4_{4,0}$ (000)	474689.257	0.016	488.1342	0.4200	1.029 (−08)	3.213 (−03)	1.167 (−02)	9.438 (−03)
$6_{2,4}$–$7_{1,7}$ (000)	488491.072	0.012	586.4792	0.1275	3.056 (−10)	1.627 (−03)	1.006 (−02)	8.836 (−03)
$7_{4,4}$–$6_{5,1}$ (010)	498502.349	0.079	2552.8797	0.8950	5.934 (−41)	1.192 (−09)	2.987 (−04)	1.367 (−03)
$8_{6,3}$–$7_{7,0}$ (000)	503568.837	0.039	1394.8142	0.9250	7.368 (−23)	4.993 (−06)	2.422 (−03)	4.194 (−03)
$8_{6,2}$–$7_{7,1}$ (000)	504482.999	0.039	1394.8141	0.3084	7.378 (−23)	5.002 (−06)	2.426 (−03)	4.201 (−03)
$14_{3,12}$–$13_{4,9}$ (000)	530342.750	0.111	2533.7932	1.4612	1.233 (−40)	1.449 (−09)	3.286 (−04)	1.481 (−03)
$5_{2,4}$–$4_{3,1}$ (010)	546690.698	0.070	2005.9170	0.9307	2.221 (−32)	6.647 (−08)	8.749 (−04)	2.532 (−03)
$1_{1,0}$–$1_{0,1}$ (000)	556935.988	0.009	23.7944	15.3568	2.071 (−01)	1.054 (−01)	3.148 (−02)	1.726 (−02)
$12_{6,7}$–$13_{3,10}$ (000)	571914.121	0.093	2414.7234	0.9787	9.422 (−39)	3.662 (−09)	4.384 (−04)	1.789 (−03)
$7_{4,3}$–$6_{5,2}$ (010)	578057.280	0.085	2552.8572	2.7059	6.599 (−41)	1.369 (−09)	3.456 (−04)	1.583 (−03)
$9_{2,8}$–$8_{3,5}$ (010)	593708.689	0.117	2670.7896	0.6418	9.665 (−43)	6.009 (−10)	2.870 (−04)	1.452 (−03)
$6_{3,4}$–$5_{4,1}$ (010)	595079.958	0.087	2251.8625	2.9024	3.390 (−36)	1.226 (−08)	6.110 (−04)	2.175 (−03)
$5_{3,2}$–$4_{4,1}$ (000)	620701.115	0.016	488.1077	1.2940	1.245 (−08)	4.131 (−03)	1.519 (−02)	1.231 (−02)
$9_{7,3}$–$8_{8,0}$ (000)	645766.054	0.063	1789.0428	0.2940	6.083 (−29)	3.694 (−07)	1.522 (−03)	3.676 (−03)
$9_{7,2}$–$8_{8,1}$ (000)	645905.564	0.063	1789.0428	0.8821	6.084 (−29)	3.695 (−07)	1.522 (−03)	3.677 (−03)
$1_{1,0}$–$1_{0,1}$ (010)	658006.475	0.063	1618.5571	14.8354	2.836 (−26)	1.281 (−06)	2.106 (−03)	4.411 (−03)
$2_{1,1}$–$2_{0,2}$ (000)	752033.132	0.010	70.0908	7.0636	4.777 (−02)	9.972 (−02)	3.889 (−02)	2.223 (−02)
$11_{5,7}$–$12_{2,10}$ (000)	766793.580	0.103	1960.2074	0.3179	1.438 (−31)	1.262 (−07)	1.324 (−03)	3.697 (−03)
$10_{5,6}$–$11_{2,9}$ (000)	841050.473	0.069	1690.6644	0.7964	2.467 (−27)	9.544 (−07)	2.352 (−03)	5.246 (−03)
$12_{5,8}$–$13_{2,11}$ (000)	854050.433	0.152	2246.8848	1.0280	5.094 (−36)	1.770 (−08)	8.780 (−04)	3.124 (−03)
$2_{1,1}$–$2_{0,2}$ (010)	859965.421	0.050	1664.9646	6.9909	6.299 (−27)	1.171 (−06)	2.517 (−03)	5.496 (−03)
$10_{8,3}$–$9_{9,0}$ (000)	863837.022	0.209	2225.4692	0.8630	1.108 (−35)	2.086 (−08)	9.227 (−04)	3.224 (−03)
$10_{8,2}$–$9_{9,1}$ (000)	863857.787	0.209	2225.4692	0.2877	1.108 (−35)	2.086 (−08)	9.227 (−04)	3.225 (−03)
$2_{0,2}$–$1_{1,1}$ (010)	899301.984	0.114	1634.9671	2.3946	1.900 (−26)	1.513 (−06)	2.775 (−03)	5.911 (−03)
$6_{2,4}$–$7_{1,7}$ (010)	902397.810	0.109	2181.0899	0.1679	5.602 (−35)	2.985 (−08)	1.043 (−03)	3.513 (−03)
$3_{1,2}$–$2_{2,1}$ (010)	902609.359	0.116	1742.3056	2.8115	4.008 (−28)	7.014 (−07)	2.296 (−03)	5.352 (−03)
$9_{2,8}$–$8_{3,5}$ (000)	906205.939	0.019	1050.1577	0.4767	2.608 (−17)	1.023 (−04)	8.004 (−03)	1.044 (−02)
$4_{2,2}$–$3_{3,1}$ (000)	916171.509	0.014	285.2193	0.5678	2.336 (−05)	2.536 (−02)	3.202 (−02)	2.197 (−02)
$6_{2,5}$–$5_{3,2}$ (010)	923113.564	0.092	2130.4943	3.5914	3.501 (−34)	4.384 (−08)	1.168 (−03)	3.771 (−03)
$6_{3,3}$–$5_{4,2}$ (010)	926187.453	0.097	2251.6953	1.0271	4.483 (−36)	1.839 (−08)	9.420 (−04)	3.368 (−03)
$8_{2,7}$–$7_{3,4}$ (010)	968047.499	0.115	2462.8752	2.7134	2.307 (−39)	4.186 (−09)	6.726 (−04)	2.873 (−03)
$5_{2,4}$–$4_{3,1}$ (000)	970315.097	0.013	383.8425	0.9219	6.938 (−07)	1.313 (−02)	2.835 (−02)	2.115 (−02)
$2_{0,2}$–$1_{1,1}$ (000)	987926.549	0.012	37.1371	2.5830	1.826 (−01)	1.616 (−01)	5.383 (−02)	3.003 (−02)
$13_{5,9}$–$14_{2,12}$ (000)	1068679.420	0.241	2550.8825	0.3476	1.024 (−40)	2.425 (−09)	6.319 (−04)	2.910 (−03)
$7_{2,6}$–$6_{3,3}$ (010)	1077763.388	0.111	2282.5896	1.1504	1.596 (−36)	1.683 (−08)	1.032 (−03)	3.796 (−03)
$3_{1,2}$–$3_{0,3}$ (000)	1097364.905	0.012	136.7617	22.2672	5.346 (−03)	8.655 (−02)	4.982 (−02)	3.026 (−02)

TABLE 4—*Continued*

Transition	ν_{ab} (MHz)	Uncertainty ($\frac{1}{2}$ σ)	E_l (cm^{-1})	$\mu^2 S$	*I* (50 K)	*I* (200 K)	*I* (800 K)	*I* (1500 K)
$11_{6,6}$–$12_{3,9}$ (000)	1101130.602	0.086	2105.8679	0.2030	9.295 (−34)	6.116 (−08)	1.448 (−03)	4.592 (−03)
$9_{5,5}$–$10_{2,8}$ (000)	1109597.594	0.040	1437.9686	0.1875	2.532 (−23)	7.518 (−06)	4.850 (−03)	8.781 (−03)
$1_{1,1}$–$0_{0,0}$ (000)	1113342.917	0.008	0.0000	3.4126	7.371 (−01)	2.345 (−01)	6.461 (−02)	3.499 (−02)
$7_{2,5}$–$8_{1,8}$ (000)..........	1146621.322	0.015	744.1627	0.2674	1.772 (−12)	1.138 (−03)	1.743 (−02)	1.764 (−02)
$3_{1,2}$–$2_{2,1}$ (000)..........	1153126.676	0.014	134.9016	3.1104	5.852 (−03)	9.159 (−02)	5.244 (−02)	3.183 (−02)
$11_{3,8}$–$12_{2,11}$ (000)	1153370.911	0.086	1774.7511	0.6005	1.414 (−28)	6.895 (−07)	2.747 (−03)	6.603 (−03)
$11_{9,3}$–$10_{10,0}$ (000)	1155166.484	0.477	2701.8885	0.2880	4.648 (−43)	8.759 (−10)	5.193 (−04)	2.718 (−03)
$11_{9,2}$–$10_{10,1}$ (000)	1155169.558	0.477	2701.8885	0.8641	4.648 (−43)	8.759 (−10)	5.193 (−04)	2.718 (−03)
$6_{3,4}$–$5_{4,1}$ (000)..........	1158323.892	0.016	610.3412	3.0156	2.193 (−10)	3.007 (−03)	2.240 (−02)	2.026 (−02)
$3_{2,1}$–$3_{1,2}$ (000)..........	1162911.700	0.010	173.3658	26.0030	1.473 (−03)	6.996 (−02)	4.934 (−02)	3.093 (−02)
$8_{5,4}$–$7_{6,1}$ (000)..........	1168358.517	0.020	1216.1945	2.6178	7.558 (−20)	3.877 (−05)	7.596 (−03)	1.143 (−02)
$7_{4,4}$–$6_{5,1}$ (000)	1172525.859	0.019	888.6326	0.9410	9.912 (−15)	4.104 (−04)	1.374 (−02)	1.570 (−02)
$8_{5,3}$–$7_{6,2}$ (000)..........	1190828.892	0.020	1216.1898	0.8742	7.625 (−20)	3.942 (−05)	7.737 (−03)	1.164 (−02)
$1_{1,1}$–$0_{0,0}$ (010)	1205789.303	0.107	1594.7463	3.2974	9.355 (−26)	2.616 (−06)	3.964 (−03)	8.197 (−03)
$4_{2,2}$–$4_{1,3}$ (000)	1207638.712	0.012	275.4970	12.4015	3.803 (−05)	3.467 (−02)	4.258 (−02)	2.910 (−02)
$3_{1,2}$–$3_{0,3}$ (010)..........	1214661.769	0.057	1731.8967	22.7706	6.760 (−28)	9.814 (−07)	3.119 (−03)	7.239 (−03)
$8_{4,5}$–$7_{5,2}$ (010)..........	1215067.641	0.119	2724.1671	4.6214	2.134 (−43)	7.795 (−10)	5.238 (−04)	2.795 (−03)
$9_{6,4}$–$8_{7,1}$ (000)..........	1215801.736	0.059	1590.6907	0.8247	1.086 (−25)	2.713 (−06)	4.025 (−03)	8.296 (−03)
$9_{6,3}$–$8_{7,2}$ (000)..........	1219944.374	0.059	1590.6900	2.4750	1.088 (−25)	2.721 (−06)	4.038 (−03)	8.324 (−03)
$7_{3,5}$–$6_{4,2}$ (010)	1222823.607	0.103	2399.1654	1.5476	2.555 (−38)	8.121 (−09)	9.455 (−04)	3.842 (−03)
$2_{2,0}$–$2_{1,1}$ (000)..........	1228788.840	0.011	95.1759	4.3124	2.514 (−02)	1.288 (−01)	5.988 (−02)	3.519 (−02)
$13_{3,11}$–$12_{4,8}$ (000).......	1271472.972	0.119	2205.6527	0.6222	2.740 (−35)	3.379 (−08)	1.390 (−03)	4.806 (−03)
$7_{4,3}$–$6_{5,2}$ (000)	1278265.923	0.018	888.5987	2.8582	1.031 (−14)	4.422 (−04)	1.493 (−02)	1.709 (−02)
$8_{2,7}$–$7_{3,4}$ (000)..........	1296411.049	0.015	842.3566	2.1147	5.471 (−14)	6.242 (−04)	1.645 (−02)	1.811 (−02)
$8_{4,5}$–$9_{1,8}$ (000)..........	1307963.287	0.023	1079.0796	0.4935	1.101 (−17)	1.145 (−04)	1.084 (−02)	1.456 (−02)
$6_{2,5}$–$5_{3,2}$ (000)..........	1322064.783	0.013	508.8121	3.3216	8.956 (−09)	6.993 (−03)	3.054 (−02)	2.542 (−02)
$10_{7,4}$–$9_{8,1}$ (000)	1335279.326	0.128	2009.8051	2.3935	3.206 (−32)	1.441 (−07)	2.073 (−03)	6.084 (−03)
$10_{7,3}$–$9_{8,2}$ (000)	1335984.734	0.128	2009.8050	0.7978	3.207 (−32)	1.442 (−07)	2.074 (−03)	6.087 (−03)
$7_{4,4}$–$8_{1,7}$ (000)..........	1344676.176	0.017	882.8903	0.1315	1.292 (−14)	4.810 (−04)	1.584 (−02)	1.806 (−02)
$14_{5,10}$–$15_{2,13}$ (000)......	1378167.571	0.378	2872.2742	1.0248	1.092 (−45)	2.990 (−10)	4.530 (−04)	2.744 (−03)
$13_{7,7}$–$14_{4,10}$ (000)	1386269.011	0.257	2880.8342	0.1842	8.046 (−46)	2.826 (−10)	4.486 (−04)	2.737 (−03)
$3_{2,1}$–$3_{1,2}$ (010)..........	1406675.550	0.091	1772.4134	24.2006	1.672 (−28)	8.309 (−07)	3.340 (−03)	8.039 (−03)
$5_{2,3}$–$5_{1,4}$ (000)..........	1410617.988	0.012	399.4575	42.9566	4.694 (−07)	1.622 (−02)	3.956 (−02)	3.008 (−02)
$4_{2,2}$–$4_{1,3}$ (010)	1421957.576	0.106	1875.4697	11.8469	4.123 (−30)	3.995 (−07)	2.803 (−03)	7.360 (−03)
$8_{4,4}$–$7_{5,3}$ (010)..........	1428471.994	0.129	2724.0414	1.5781	2.290 (−43)	8.953 (−10)	6.121 (−04)	3.276 (−03)
$9_{4,6}$–$10_{1,9}$ (000)	1435008.375	0.040	1293.0181	0.1777	5.194 (−21)	2.658 (−05)	8.062 (−03)	1.298 (−02)
$7_{2,6}$–$6_{3,3}$ (000)	1440781.665	0.013	661.5489	0.9729	3.808 (−11)	2.506 (−03)	2.520 (−02)	2.389 (−02)
$5_{2,3}$–$4_{3,2}$ (010)	1473570.467	0.113	2004.8157	4.1321	3.984 (−32)	1.623 (−07)	2.299 (−03)	6.731 (−03)
$2_{2,0}$–$2_{1,1}$ (010)..........	1494057.486	0.081	1693.6499	3.9989	2.907 (−27)	1.540 (−06)	4.076 (−03)	9.196 (−03)
$11_{8,4}$–$10_{9,1}$ (000)	1529130.687	0.249	2471.2550	0.7896	2.087 (−39)	5.839 (−09)	1.029 (−03)	4.462 (−03)
$11_{8,3}$–$10_{9,2}$ (000)	1529245.716	0.248	2471.2550	2.3689	2.087 (−39)	5.840 (−09)	1.029 (−03)	4.462 (−03)
$6_{3,3}$–$5_{4,2}$ (000)..........	1541967.050	0.015	610.1144	1.0979	2.482 (−10)	3.838 (−03)	2.949 (−02)	2.681 (−02)
$6_{4,3}$–$7_{1,6}$ (000)..........	1574232.067	0.014	704.2140	0.2449	8.469 (−12)	1.984 (−03)	2.540 (−02)	2.500 (−02)
$5_{2,3}$–$5_{1,4}$ (010)..........	1592068.265	0.116	2000.8630	42.7077	4.718 (−32)	1.780 (−07)	2.493 (−03)	7.287 (−03)
$8_{5,4}$–$9_{2,7}$ (000)..........	1596252.461	0.023	1201.9215	0.3118	1.429 (−19)	5.592 (−05)	1.051 (−02)	1.572 (−02)
$4_{1,3}$–$4_{0,4}$ (000)	1602219.342	0.011	222.0528	6.9404	2.901 (−04)	6.461 (−02)	6.147 (−02)	4.039 (−02)
$3_{0,3}$–$2_{1,2}$ (010)..........	1643919.328	0.109	1677.0614	16.5369	5.453 (−27)	1.877 (−06)	4.601 (−03)	1.026 (−02)
$7_{2,5}$–$8_{1,8}$ (010)..........	1646632.434	0.122	2337.6668	0.3481	2.613 (−37)	1.622 (−08)	1.404 (−03)	5.451 (−03)
$2_{2,1}$–$2_{1,2}$ (000)..........	1661007.762	0.011	79.4964	8.5508	4.949 (−02)	1.856 (−01)	8.221 (−02)	4.796 (−02)
$2_{1,2}$–$1_{0,1}$ (000)..........	1669904.752	0.009	23.7944	15.3477	3.676 (−01)	2.782 (−01)	9.133 (−02)	5.085 (−02)
$10_{4,7}$–$11_{1,10}$ (000)	1693469.742	0.071	1524.8479	0.5314	1.314 (−24)	5.749 (−06)	6.223 (−03)	1.222 (−02)
$4_{3,2}$–$5_{0,5}$ (000)..........	1713882.952	0.012	325.3479	0.1144	7.213 (−06)	3.246 (−02)	5.443 (−02)	3.906 (−02)
$3_{0,3}$–$2_{1,2}$ (000)..........	1716769.533	0.011	79.4964	17.8475	4.999 (−02)	1.906 (−01)	8.483 (−02)	4.952 (−02)
$5_{3,3}$–$6_{0,6}$ (000)	1716956.616	0.013	446.6966	0.0561	9.177 (−08)	1.358 (−02)	4.383 (−02)	3.482 (−02)
$4_{1,3}$–$4_{0,4}$ (010)	1739351.281	0.066	1817.4512	7.2464	3.557 (−29)	7.158 (−07)	3.771 (−03)	9.470 (−03)
$8_{3,6}$–$7_{4,3}$ (010)..........	1740397.563	0.133	2572.1391	5.9464	5.777 (−41)	3.141 (−09)	9.710 (−04)	4.594 (−03)
$2_{1,2}$–$1_{0,1}$ (010)..........	1753915.445	0.111	1618.5571	14.8282	4.562 (−26)	3.014 (−06)	5.435 (−03)	1.155 (−02)
$6_{3,3}$–$6_{2,4}$ (000)	1762042.660	0.012	602.7735	16.3527	3.372 (−10)	4.512 (−03)	3.393 (−02)	3.075 (−02)
$7_{3,5}$–$6_{4,2}$ (000)	1766198.743	0.015	757.7802	1.5662	1.278 (−12)	1.482 (−03)	2.573 (−02)	2.656 (−02)
$12_{9,4}$–$11_{10,1}$ (000)	1794632.021	0.522	2972.8273	2.3932	3.207 (−47)	1.803 (−10)	4.863 (−04)	3.223 (−03)
$12_{9,3}$–$11_{10,2}$ (000)	1794650.403	0.523	2972.8273	0.7978	3.207 (−47)	1.803 (−10)	4.863 (−04)	3.223 (−03)
$6_{2,4}$–$6_{1,5}$ (000)	1794788.923	0.011	542.9058	14.3411	2.920 (−09)	7.043 (−03)	3.845 (−02)	3.315 (−02)
$7_{3,4}$–$7_{2,5}$ (000)..........	1797158.733	0.013	782.4098	60.0582	5.298 (−13)	1.259 (−03)	2.502 (−02)	2.638 (−02)
$4_{1,3}$–$3_{2,2}$ (010)..........	1849183.592	0.113	1813.7876	2.5494	4.128 (−29)	7.718 (−07)	4.022 (−03)	1.009 (−02)
$10_{6,5}$–$11_{3,8}$ (000)	1851205.596	0.064	1813.2234	0.3073	4.214 (−29)	7.756 (−07)	4.031 (−03)	1.010 (−02)
$5_{3,2}$–$5_{2,3}$ (000)..........	1867748.467	0.011	446.5107	35.1483	9.462 (−08)	1.455 (−02)	4.748 (−02)	3.780 (−02)

TABLE 4—*Continued*

Transition	ν_{ab} (MHz)	Uncertainty ($\frac{1}{2}$ σ)	E_l (cm^{-1})	$\mu^2 S$	I (50 K)	I (200 K)	I (800 K)	I (1500 K)
$8_{2,6}$–$9_{1,9}$ (000)	1879750.121	0.020	920.2100	0.0691	3.774 (−15)	4.841 (−04)	2.038 (−02)	2.415 (−02)
$6_{3,4}$–$7_{0,7}$ (000)	1880752.361	0.015	586.2435	0.1898	6.222 (−10)	5.352 (−03)	3.717 (−02)	3.328 (−02)
$8_{4,5}$–$7_{5,2}$ (000)	1884887.913	0.017	1059.8354	4.8219	2.488 (−17)	1.777 (−04)	1.589 (−02)	2.118 (−02)
$3_{3,1}$–$4_{0,4}$ (000)	1893686.545	0.014	222.0528	0.0143	3.047 (−04)	7.392 (−02)	7.203 (−02)	4.751 (−02)
$9_{4,6}$–$8_{5,3}$ (010)	1894418.074	0.164	2920.1320	2.2030	2.166 (−46)	2.749 (−10)	5.627 (−04)	3.573 (−03)
$9_{5,5}$–$8_{6,2}$ (000)	1898852.244	0.024	1411.6419	1.5429	7.961 (−23)	1.422 (−05)	8.501 (−03)	1.522 (−02)
$12_{3,9}$–$13_{2,12}$ (000)......	1903497.257	0.161	2042.3741	0.1737	1.117 (−32)	1.525 (−07)	2.740 (−03)	8.331 (−03)
$12_{3,10}$–$11_{4,7}$ (000)......	1903643.698	0.101	1899.0082	2.5376	1.940 (−30)	4.278 (−07)	3.547 (−03)	9.560 (−03)
$5_{2,3}$–$4_{3,2}$ (000)	1918485.441	0.012	382.5169	4.5857	9.521 (−07)	2.354 (−02)	5.464 (−02)	4.125 (−02)
$3_{2,2}$–$3_{1,3}$ (000)	1919359.520	0.010	142.2785	4.4203	5.391 (−03)	1.326 (−01)	8.421 (−02)	5.196 (−02)
$10_{6,5}$–$9_{7,2}$ (000)	1930215.966	0.074	1810.5879	4.4555	4.684 (−29)	8.170 (−07)	4.213 (−03)	1.055 (−02)
$7_{3,4}$–$6_{4,3}$ (010)	1933474.781	0.118	2398.3815	5.4505	3.080 (−38)	1.192 (−08)	1.466 (−03)	6.011 (−03)
$10_{6,4}$–$9_{7,3}$ (000)	1945009.917	0.077	1810.5833	1.4864	4.694 (−29)	8.219 (−07)	4.243 (−03)	1.062 (−02)
$6_{2,4}$–$6_{1,5}$ (010)	1946460.306	0.120	2146.2637	14.8293	2.678 (−34)	7.350 (−08)	2.322 (−03)	7.705 (−03)
$2_{2,1}$–$2_{1,2}$ (010)	1955971.738	0.071	1677.0614	8.2606	5.728 (−27)	2.157 (−06)	5.424 (−03)	1.214 (−02)
$9_{5,4}$–$8_{6,3}$ (000)	1969214.416	0.024	1411.6114	4.6568	8.044 (−23)	1.464 (−05)	8.798 (−03)	1.577 (−02)
$5_{4,2}$–$6_{1,5}$ (000)	2014864.532	0.014	542.9058	0.0334	3.009 (−09)	7.716 (−03)	4.288 (−02)	3.709 (−02)
$8_{3,5}$–$8_{2,6}$ (000)	2015982.847	0.015	982.9117	21.5977	4.026 (−16)	3.258 (−04)	1.945 (−02)	2.433 (−02)
$11_{7,5}$–$10_{8,2}$ (000).......	2024457.394	0.165	2254.2844	1.4553	5.552 (−36)	3.484 (−08)	1.984 (−03)	7.217 (−03)
$11_{7,4}$–$10_{8,3}$ (000).......	2027255.529	0.164	2254.2837	4.3666	5.554 (−36)	3.488 (−08)	1.986 (−03)	7.226 (−03)
$4_{3,1}$–$4_{2,2}$ (000)	2040476.759	0.011	315.7795	7.4297	1.066 (−05)	3.993 (−02)	6.529 (−02)	4.668 (−02)
$11_{4,8}$–$12_{1,11}$ (000)......	2050980.055	0.124	1774.6163	0.1699	1.734 (−28)	1.110 (−06)	4.759 (−03)	1.158 (−02)
$4_{1,3}$–$3_{2,2}$ (000)	2074432.382	0.012	206.3014	2.8729	5.491 (−04)	8.890 (−02)	8.074 (−02)	5.269 (−02)
$9_{3,7}$–$8_{4,4}$ (010)	2090772.019	0.158	2771.6901	2.1278	4.624 (−44)	8.638 (−10)	8.064 (−04)	4.532 (−03)
$7_{3,4}$–$7_{2,5}$ (010)	2107022.663	0.125	2392.5925	57.1509	3.871 (−38)	1.329 (−08)	1.606 (−03)	6.569 (−03)
$6_{3,3}$–$6_{2,4}$ (010)	2140487.032	0.100	2211.1906	15.0451	2.649 (−35)	4.959 (−08)	2.259 (−03)	7.938 (−03)
$8_{4,4}$–$7_{5,3}$ (000)	2162370.498	0.017	1059.6466	1.6709	2.588 (−17)	1.980 (−04)	1.809 (−02)	2.419 (−02)
$3_{1,3}$–$2_{0,2}$ (000)	2164132.001	0.010	70.0908	7.3550	7.438 (−02)	2.447 (−01)	1.073 (−01)	6.255 (−02)
$7_{3,5}$–$8_{0,8}$ (000)	2177409.704	0.016	744.0637	0.0628	2.205 (−12)	1.927 (−03)	3.212 (−02)	3.296 (−02)
$12_{8,5}$–$11_{9,2}$ (000).......	2191225.490	0.313	2740.4208	4.3644	1.438 (−43)	1.121 (−09)	8.914 (−04)	4.887 (−03)
$12_{8,4}$–$11_{9,3}$ (000).......	2191723.253	0.308	2740.4207	1.4549	1.438 (−43)	1.121 (−09)	8.916 (−04)	4.888 (−03)
$3_{3,0}$–$3_{2,1}$ (000)	2196345.790	0.012	212.1564	11.3059	4.503 (−04)	8.904 (−02)	8.429 (−02)	5.537 (−02)
$10_{3,8}$–$9_{4,5}$ (010)	2217265.507	0.200	2998.7663	5.8441	1.328 (−47)	1.764 (−10)	5.663 (−04)	3.858 (−03)
$5_{1,4}$–$5_{0,5}$ (000)	2221750.406	0.012	325.3479	19.4139	7.696 (−06)	3.978 (−02)	6.951 (−02)	5.022 (−02)
$3_{2,2}$–$3_{1,3}$ (010)	2227574.164	0.053	1739.4837	4.3281	6.244 (−28)	1.522 (−06)	5.477 (−03)	1.297 (−02)
$3_{1,3}$–$2_{0,2}$ (010)	2234026.771	0.095	1664.9646	7.0483	9.116 (−27)	2.607 (−06)	6.280 (−03)	1.397 (−02)
$8_{3,6}$–$7_{4,3}$ (000)	2244811.054	0.017	931.2371	5.7304	2.644 (−15)	5.130 (−04)	2.360 (−02)	2.837 (−02)
$8_{3,5}$–$8_{2,6}$ (010)	2247746.017	0.145	2595.8129	21.5405	2.624 (−41)	3.235 (−09)	1.184 (−03)	5.754 (−03)
$4_{2,3}$–$4_{1,4}$ (000)	2264149.558	0.011	224.8384	15.9562	2.871 (−04)	8.316 (−02)	8.477 (−02)	5.632 (−02)
$5_{3,2}$–$5_{2,3}$ (010)	2294179.491	0.089	2053.9687	32.0786	7.677 (−33)	1.620 (−07)	3.198 (−03)	9.868 (−03)
$8_{4,5}$–$9_{1,8}$ (010)	2296935.416	0.148	2688.0799	0.4914	9.538 (−43)	1.693 (−09)	1.023 (−03)	5.378 (−03)
$7_{5,3}$–$8_{2,6}$ (000)	2300455.716	0.016	982.9117	0.0419	4.140 (−16)	3.603 (−04)	2.201 (−02)	2.764 (−02)
$9_{4,5}$–$9_{3,6}$ (000)	2317882.104	0.019	1282.9191	71.7068	8.531 (−21)	4.186 (−05)	1.292 (−02)	2.088 (−02)
$4_{0,4}$–$3_{1,3}$ (010)	2337406.476	0.090	1739.4837	9.0340	6.301 (−28)	1.578 (−06)	5.729 (−03)	1.358 (−02)
$7_{2,5}$–$7_{1,6}$ (000)	2344250.362	0.013	704.2140	40.4877	9.379 (−12)	2.713 (−03)	3.697 (−02)	3.677 (−02)
$10_{4,6}$–$10_{3,7}$ (000).......	2347482.039	0.034	1538.1495	27.4357	8.808 (−25)	6.737 (−06)	8.261 (−03)	1.655 (−02)
$11_{3,9}$–$10_{4,6}$ (000).......	2356835.957	0.068	1616.4530	1.1816	5.272 (−26)	3.847 (−06)	7.203 (−03)	1.541 (−02)
$3_{3,1}$–$3_{2,2}$ (000)	2365899.585	0.012	206.3014	3.5691	5.637 (−04)	9.820 (−02)	9.130 (−02)	5.982 (−02)
$12_{7,6}$–$13_{4,9}$ (000).......	2368560.214	0.188	2533.7932	0.2686	2.466 (−40)	5.256 (−09)	1.390 (−03)	6.423 (−03)
$9_{4,5}$–$8_{5,4}$ (010)	2372359.855	0.165	2919.6329	7.0506	2.316 (−46)	3.279 (−10)	6.955 (−04)	4.443 (−03)
$7_{4,4}$–$8_{1,7}$ (010)	2372974.395	0.136	2490.3540	0.1207	1.177 (−39)	7.194 (−09)	1.505 (−03)	6.708 (−03)
$4_{0,4}$–$3_{1,3}$ (000)	2391572.560	0.011	142.2785	9.6574	5.650 (−03)	1.569 (−01)	1.035 (−01)	6.427 (−02)
$5_{1,4}$–$5_{0,5}$ (010)	2401232.209	0.091	1920.7665	20.2743	9.323 (−31)	4.369 (−07)	4.240 (−03)	1.172 (−02)
$9_{4,6}$–$10_{1,9}$ (010)	2403645.199	0.170	2903.1460	0.1882	4.201 (−46)	3.728 (−10)	7.252 (−04)	4.571 (−03)
$9_{3,6}$–$9_{2,7}$ (000)	2428247.324	0.022	1201.9215	63.7149	1.584 (−19)	7.760 (−05)	1.561 (−02)	2.360 (−02)
$8_{4,4}$–$8_{3,5}$ (000)	2446843.367	0.015	1050.1577	19.1211	3.726 (−17)	2.325 (−04)	2.065 (−02)	2.750 (−02)
$4_{3,2}$–$4_{2,3}$ (000)	2462932.987	0.010	300.3623	19.0025	1.926 (−05)	5.142 (−02)	8.003 (−02)	5.681 (−02)
$12_{4,9}$–$13_{1,12}$ (000)......	2477509.147	0.197	2042.3106	0.4816	1.183 (−32)	1.865 (−07)	3.508 (−03)	1.075 (−02)
$7_{2,5}$–$7_{1,6}$ (010)	2484151.505	0.128	2309.7302	42.7282	7.866 (−37)	2.729 (−08)	2.174 (−03)	8.336 (−03)
$4_{3,1}$–$4_{2,2}$ (010)	2488754.367	0.087	1922.9011	6.8665	8.685 (−31)	4.417 (−07)	4.366 (−03)	1.210 (−02)
$8_{2,6}$–$9_{1,9}$ (010)	2501384.400	0.160	2512.3757	0.0876	5.378 (−40)	6.383 (−09)	1.520 (−03)	6.909 (−03)
$4_{3,2}$–$5_{0,5}$ (010)	2519730.008	0.097	1920.7665	0.1086	9.396 (−31)	4.526 (−07)	4.434 (−03)	1.227 (−02)
$9_{3,7}$–$8_{4,4}$ (000)	2531917.714	0.021	1131.7756	1.9010	1.989 (−18)	1.325 (−04)	1.841 (−02)	2.628 (−02)
$5_{3,3}$–$6_{0,6}$ (010)	2537059.710	0.108	2041.7805	0.0574	1.211 (−32)	1.905 (−07)	3.589 (−03)	1.100 (−02)
$6_{2,4}$–$5_{3,3}$ (010)	2541727.556	0.116	2126.4077	2.6323	5.769 (−34)	1.037 (−07)	3.088 (−03)	1.016 (−02)
$9_{4,6}$–$8_{5,3}$ (000)	2547436.478	0.023	1255.9115	2.2607	2.290 (−20)	5.450 (−05)	1.481 (−02)	2.347 (−02)

TABLE 4—*Continued*

Transition	ν_{ab} (MHz)	Uncertainty ($\frac{1}{2}$ σ)	E_l (cm^{-1})	$\mu^2 S$	I (50 K)	I (200 K)	I (800 K)	I (1500 K)
$7_{3,4}$–$6_{4,3}$ (000)	2567177.028	0.014	756.7248	5.9475	1.440 (−12)	1.988 (−03)	3.660 (−02)	3.816 (−02)
$11_{4,7}$–$11_{3,8}$ (000)	2571762.517	0.067	1813.2234	86.2552	4.511 (−29)	9.958 (−07)	5.483 (−03)	1.387 (−02)
$10_{3,8}$–$9_{4,5}$ (000)	2575004.418	0.038	1360.2353	4.7652	5.380 (−22)	2.593 (−05)	1.240 (−02)	2.145 (−02)
$8_{3,6}$–$9_{0,9}$ (000)..........	2576644.138	0.020	920.1683	0.1768	4.030 (−15)	6.151 (−04)	2.737 (−02)	3.274 (−02)
$9_{3,6}$–$9_{2,7}$ (010)..........	2586380.182	0.173	2818.3980	66.2964	8.959 (−45)	7.235 (−10)	9.039 (−04)	5.319 (−03)
$4_{2,3}$–$4_{1,4}$ (010)	2590791.891	0.063	1821.5968	15.8430	3.342 (−29)	9.426 (−07)	5.437 (−03)	1.386 (−02)
$13_{3,10}$–$14_{2,13}$ (000)......	2602481.851	0.244	2327.9140	0.4726	4.119 (−37)	2.476 (−08)	2.197 (−03)	8.566 (−03)
$10_{5,6}$–$9_{6,3}$ (000)	2618261.548	0.039	1631.3830	6.8434	3.134 (−26)	3.732 (−06)	7.730 (−03)	1.681 (−02)
$9_{2,7}$–$10_{1,10}$ (000)	2619333.979	0.044	1114.5499	0.1742	3.714 (−18)	1.537 (−04)	1.959 (−02)	2.760 (−02)
$5_{3,3}$–$5_{2,4}$ (000)..........	2630959.374	0.011	416.2087	8.4864	3.015 (−07)	2.344 (−02)	6.907 (−02)	5.416 (−02)
$4_{1,4}$–$3_{0,3}$ (000)..........	2640473.971	0.011	136.7617	30.7215	6.997 (−03)	1.755 (−01)	1.146 (−01)	7.105 (−02)
$11_{6,6}$–$10_{7,3}$ (000)	2645039.630	0.095	2054.3687	2.2430	7.744 (−33)	1.793 (−07)	3.647 (−03)	1.131 (−02)
$3_{3,0}$–$3_{2,1}$ (010)..........	2646587.083	0.062	1819.3351	10.6126	3.636 (−29)	9.728 (−07)	5.568 (−03)	1.418 (−02)
$4_{4,1}$–$5_{1,4}$ (000)..........	2657665.340	0.016	399.4575	0.0201	5.515 (−07)	2.664 (−02)	7.185 (−02)	5.557 (−02)
$6_{4,3}$–$7_{1,6}$ (010)..........	2657699.387	0.129	2309.7302	0.2041	7.945 (−37)	2.865 (−08)	2.314 (−03)	8.894 (−03)
$7_{4,3}$–$7_{3,4}$ (000)..........	2664570.784	0.013	842.3566	43.3807	6.652 (−14)	1.103 (−03)	3.247 (−02)	3.643 (−02)
$5_{2,4}$–$5_{1,5}$ (000)..........	2685638.921	0.011	326.6255	5.7894	7.585 (−06)	4.532 (−02)	8.270 (−02)	6.019 (−02)
$4_{1,4}$–$3_{0,3}$ (010)..........	2689141.309	0.090	1731.8967	29.2361	8.462 (−28)	1.846 (−06)	6.613 (−03)	1.566 (−02)
$11_{6,5}$–$10_{7,4}$ (000)	2689170.032	0.117	2054.3452	6.7504	7.768 (−33)	1.814 (−07)	3.703 (−03)	1.149 (−02)
$3_{3,1}$–$4_{0,4}$ (010)	2698138.154	0.098	1817.4512	0.0124	3.901 (−29)	9.997 (−07)	5.687 (−03)	1.447 (−02)
$12_{7,6}$–$11_{8,3}$ (000)	2714161.593	0.206	2522.2651	6.6791	3.812 (−40)	6.305 (−09)	1.610 (−03)	7.401 (−03)
$12_{7,5}$–$11_{8,4}$ (000)	2723413.666	0.224	2522.2613	2.2272	3.815 (−40)	6.320 (−09)	1.615 (−03)	7.425 (−03)
$6_{3,4}$–$7_{0,7}$ (010)..........	2730190.159	0.114	2180.6429	0.2054	8.283 (−35)	7.393 (−08)	2.992 (−03)	1.033 (−02)
$2_{2,1}$–$1_{1,0}$ (000)..........	2773976.526	0.008	42.3717	15.3993	2.100 (−01)	3.584 (−01)	1.421 (−01)	8.155 (−02)
$5_{1,4}$–$4_{2,3}$ (010)	2783473.884	0.116	1908.0163	14.8199	1.507 (−30)	5.327 (−07)	4.973 (−03)	1.367 (−02)
$9_{6,4}$–$10_{3,7}$ (000)	2790947.707	0.037	1538.1495	0.0417	9.040 (−25)	7.637 (−06)	9.696 (−03)	1.954 (−02)
$10_{5,5}$–$9_{6,4}$ (000)	2801857.636	0.042	1631.2455	2.3229	3.177 (−26)	3.919 (−06)	8.230 (−03)	1.793 (−02)
$3_{3,1}$–$3_{2,2}$ (010)..........	2807970.466	0.042	1813.7876	3.3920	4.473 (−29)	1.056 (−06)	5.939 (−03)	1.508 (−02)
$9_{4,5}$–$9_{3,6}$ (010)..........	2820925.179	0.168	2904.6704	65.4558	4.069 (−46)	4.137 (−10)	8.384 (−04)	5.321 (−03)
$12_{5,7}$–$12_{4,8}$ (000)	2848995.792	0.089	2205.6527	31.0801	3.387 (−35)	6.363 (−08)	2.974 (−03)	1.050 (−02)
$13_{5,8}$–$13_{4,9}$ (000)	2864256.164	0.161	2533.7932	103.587	2.535 (−40)	6.026 (−09)	1.657 (−03)	7.706 (−03)
$6_{3,4}$–$6_{2,5}$ (000)	2880025.294	0.013	552.9114	30.1032	2.232 (−09)	9.346 (−03)	5.870 (−02)	5.180 (−02)
$6_{1,5}$–$6_{0,6}$ (000)	2884278.885	0.012	446.6966	6.2551	1.019 (−07)	2.009 (−02)	7.115 (−02)	5.743 (−02)
$6_{4,2}$–$6_{3,3}$ (000)	2884941.040	0.011	661.5489	10.5528	4.485 (−11)	4.283 (−03)	4.836 (−02)	4.675 (−02)
$4_{3,2}$–$4_{2,3}$ (010)	2901971.683	0.052	1908.0163	18.1610	1.514 (−30)	5.484 (−07)	5.167 (−03)	1.422 (−02)
$13_{4,10}$–$14_{1,13}$ (000)......	2947342.726	0.276	2327.8837	0.1516	4.188 (−37)	2.704 (−08)	2.463 (−03)	9.649 (−03)
$6_{2,4}$–$5_{3,3}$ (000)..........	2962111.192	0.013	503.9681	3.0060	1.302 (−08)	1.355 (−02)	6.577 (−02)	5.576 (−02)
$2_{2,0}$–$1_{1,1}$ (000)..........	2968748.520	0.008	37.1371	4.2551	2.555 (−01)	3.901 (−01)	1.526 (−01)	8.744 (−02)
$5_{1,4}$–$4_{2,3}$ (000)	2970800.440	0.012	300.3623	16.8476	1.974 (−05)	5.874 (−02)	9.511 (−02)	6.798 (−02)
$5_{0,5}$–$4_{1,4}$ (010)	2973033.566	0.081	1821.5968	37.7312	3.399 (−29)	1.038 (−06)	6.171 (−03)	1.581 (−02)
$12_{4,8}$–$12_{3,9}$ (000)	2991473.560	0.112	2105.8679	28.1269	1.233 (−33)	1.349 (−07)	3.722 (−03)	1.211 (−02)
$11_{5,6}$–$11_{4,7}$ (000)	2997538.796	0.062	1899.0082	78.8121	2.101 (−30)	5.983 (−07)	5.409 (−03)	1.479 (−02)
$8_{2,6}$–$8_{1,7}$ (000)..........	2998565.616	0.016	882.8903	12.7491	1.570 (−14)	8.948 (−04)	3.364 (−02)	3.922 (−02)
$10_{3,7}$–$10_{2,8}$ (000)	3003347.597	0.040	1437.9686	20.0636	3.347 (−23)	1.652 (−05)	1.242 (−02)	2.307 (−02)
$15_{4,12}$–$14_{5,9}$ (000).......	3011981.501	0.433	2983.3963	1.3618	2.414 (−47)	2.457 (−10)	7.727 (−04)	5.253 (−03)
$5_{0,5}$–$4_{1,4}$ (000)	3013199.593	0.011	224.8384	39.9373	2.991 (−04)	1.021 (−01)	1.104 (−01)	7.408 (−02)
$8_{4,4}$–$8_{3,5}$ (010)..........	3024920.029	0.127	2670.7896	17.2661	1.847 (−42)	2.335 (−09)	1.361 (−03)	7.118 (−03)
$8_{5,4}$–$9_{2,7}$ (010)..........	3034945.506	0.169	2818.3980	0.2240	9.134 (−45)	8.094 (−10)	1.047 (−03)	6.198 (−03)
$8_{3,5}$–$7_{4,4}$ (010)..........	3036348.078	0.139	2569.5080	2.8420	7.059 (−41)	4.852 (−09)	1.639 (−03)	7.873 (−03)
$5_{2,4}$–$5_{1,5}$ (010)..........	3037605.104	0.085	1922.8290	5.8178	8.931 (−31)	5.087 (−07)	5.245 (−03)	1.464 (−02)
$5_{4,1}$–$5_{3,2}$ (000)..........	3043766.185	0.012	508.8121	21.4768	1.097 (−08)	1.333 (−02)	6.684 (−02)	5.696 (−02)
$9_{3,7}$–$10_{0,10}$ (000)	3048859.624	0.045	1114.5322	0.0542	3.784 (−18)	1.710 (−04)	2.252 (−02)	3.191 (−02)
$2_{2,1}$–$1_{1,0}$ (010)..........	3051880.708	0.113	1640.5059	14.8797	2.298 (−26)	3.890 (−06)	8.753 (−03)	1.929 (−02)
$5_{3,3}$–$5_{2,4}$ (010)..........	3065530.020	0.074	2024.1526	8.1968	2.336 (−32)	2.469 (−07)	4.408 (−03)	1.340 (−02)
$7_{3,5}$–$8_{0,8}$ (010)..........	3072608.565	0.119	2337.4633	0.0707	2.979 (−37)	2.596 (−08)	2.514 (−03)	9.947 (−03)
$14_{5,9}$–$14_{4,10}$ (000).......	3074733.516	0.275	2880.8342	35.7516	9.679 (−46)	5.211 (−10)	9.469 (−04)	5.911 (−03)
$10_{4,7}$–$9_{5,4}$ (000)	3118999.242	0.039	1477.2974	8.2985	8.163 (−24)	1.277 (−05)	1.197 (−02)	2.303 (−02)
$4_{4,0}$–$4_{3,1}$ (000)	3126585.214	0.015	383.8425	3.7966	9.850 (−07)	3.336 (−02)	8.575 (−02)	6.587 (−02)
$6_{1,5}$–$6_{0,6}$ (010)	3132326.961	0.115	2041.7805	6.4769	1.241 (−32)	2.207 (−07)	4.355 (−03)	1.345 (−02)
$5_{1,5}$–$4_{0,4}$ (000)	3135010.989	0.011	222.0528	13.5189	3.319 (−04)	1.070 (−01)	1.150 (−01)	7.713 (−02)
$9_{4,5}$–$8_{5,4}$ (000)..........	3149876.967	0.019	1255.1667	7.5432	2.412 (−20)	6.354 (−05)	1.801 (−02)	2.876 (−02)
$5_{1,5}$–$4_{0,4}$ (010)	3159148.818	0.097	1817.4512	12.8548	3.969 (−29)	1.115 (−06)	6.570 (−03)	1.682 (−02)
$5_{4,2}$–$6_{1,5}$ (010)	3160759.885	0.128	2146.2637	0.0253	2.898 (−34)	1.047 (−07)	3.639 (−03)	1.228 (−02)
$8_{2,6}$–$8_{1,7}$ (010)..........	3161576.457	0.147	2490.3540	13.4260	1.221 (−39)	8.811 (−09)	1.960 (−03)	8.827 (−03)
$4_{4,1}$–$4_{3,2}$ (000)	3165532.793	0.015	382.5169	11.3298	1.034 (−06)	3.396 (−02)	8.693 (−02)	6.674 (−02)
$6_{2,5}$–$6_{1,6}$ (000)	3167578.134	0.011	447.2524	18.0370	1.008 (−07)	2.132 (−02)	7.742 (−02)	6.276 (−02)

TABLE 4—*Continued*

Transition	ν_{ab} (MHz)	Uncertainty ($\frac{1}{2}$ σ)	E_l (cm^{-1})	$\mu^2 S$	I (50 K)	I (200 K)	I (800 K)	I (1500 K)
$5_{4,2}-5_{3,3}$ (000)	3182186.801	0.012	503.9681	7.0043	1.311 (−08)	1.422 (−02)	7.021 (−02)	5.970 (−02)
$6_{5,2}-7_{2,5}$ (000)	3183463.594	0.016	782.4098	0.0344	5.860 (−13)	1.919 (−03)	4.257 (−02)	4.572 (−02)
$7_{3,5}-7_{2,6}$ (000)	3210358.118	0.014	709.6082	11.0338	8.044 (−12)	3.259 (−03)	4.889 (−02)	4.942 (−02)
$6_{4,3}-6_{3,4}$ (000)	3230146.418	0.012	648.9787	29.6233	7.126 (−11)	5.061 (−03)	5.483 (−02)	5.269 (−02)
$14_{3,11}-15_{2,14}$ (000)	3242105.141	0.345	2631.2835	0.1468	7.696 (−42)	3.251 (−09)	1.556 (−03)	7.897 (−03)
$10_{5,5}-10_{4,6}$ (000)	3245323.304	0.039	1616.4530	21.4177	5.489 (−26)	4.819 (−06)	9.665 (−03)	2.092 (−02)
$2_{2,0}-1_{1,1}$ (010)	3253324.891	0.127	1634.9671	4.2116	2.821 (−26)	4.224 (−06)	9.369 (−03)	2.060 (−02)
$7_{4,3}-7_{3,4}$ (010)	3275649.115	0.095	2462.8752	39.6415	3.292 (−39)	1.099 (−08)	2.127 (−03)	9.372 (−03)
$11_{5,7}-10_{6,4}$ (000)	3307403.060	0.072	1875.4618	3.0218	4.944 (−30)	7.570 (−07)	6.171 (−03)	1.662 (−02)
$6_{3,4}-6_{2,5}$ (010)	3310494.176	0.094	2161.2860	29.4571	1.695 (−34)	9.691 (−08)	3.693 (−03)	1.264 (−02)
$10_{2,8}-11_{1,11}$ (000)	3323228.600	0.086	1327.1176	0.0514	1.821 (−21)	3.923 (−05)	1.661 (−02)	2.824 (−02)
$7_{4,4}-7_{3,5}$ (000)	3329185.202	0.013	816.6942	12.3673	1.713 (−13)	1.545 (−03)	4.168 (−02)	4.616 (−02)
$3_{2,2}-2_{1,1}$ (000)	3331458.390	0.012	95.1759	5.6980	3.200 (−02)	2.775 (−01)	1.527 (−01)	9.229 (−02)
$12_{6,7}-11_{7,4}$ (000)	3354519.723	0.137	2321.9057	9.1761	5.252 (−37)	3.078 (−08)	2.800 (−03)	1.097 (−02)
$9_{2,7}-10_{1,10}$ (010)	3395402.766	0.194	2705.1396	0.2152	5.420 (−43)	1.969 (−09)	1.421 (−03)	7.686 (−03)
$13_{7,7}-12_{8,4}$ (000)	3404037.769	0.270	2813.5287	3.0796	1.099 (−44)	9.045 (−10)	1.172 (−03)	6.944 (−03)
$13_{7,6}-12_{8,5}$ (000)	3430497.381	0.328	2813.5122	9.2526	1.100 (−44)	9.092 (−10)	1.180 (−03)	6.995 (−03)
$14_{4,11}-15_{1,14}$ (000)	3440256.583	0.384	2631.2689	0.4321	7.734 (−42)	3.379 (−09)	1.642 (−03)	8.354 (−03)
$12_{6,6}-11_{7,5}$ (000)	3468263.974	0.172	2321.8131	3.0860	5.282 (−37)	3.147 (−08)	2.886 (−03)	1.133 (−02)
$11_{7,5}-12_{4,8}$ (000)	3482398.878	0.144	2205.6527	0.0386	3.448 (−35)	7.277 (−08)	3.569 (−03)	1.271 (−02)
$6_{4,2}-6_{3,3}$ (010)	3494856.587	0.085	2282.5896	9.8130	2.166 (−36)	4.194 (−08)	3.118 (−03)	1.185 (−02)
$8_{4,5}-8_{3,6}$ (000)	3495358.205	0.016	1006.1159	43.1577	1.889 (−16)	4.081 (−04)	3.097 (−02)	4.031 (−02)
$14_{4,11}-13_{5,8}$ (000)	3498248.829	0.281	2629.3345	5.4299	8.300 (−42)	3.464 (−09)	1.673 (−03)	8.502 (−03)
$9_{5,4}-9_{4,5}$ (000)	3509431.283	0.020	1360.2353	51.8201	5.553 (−22)	3.202 (−05)	1.644 (−02)	2.881 (−02)
$8_{3,6}-9_{0,9}$ (010)	3534844.077	0.146	2512.2828	0.2040	5.596 (−40)	8.093 (−09)	2.084 (−03)	9.607 (−03)
$7_{1,6}-7_{0,7}$ (000)	3536666.711	0.014	586.2435	18.5700	6.850 (−10)	8.430 (−03)	6.661 (−02)	6.097 (−02)
$14_{6,8}-14_{5,9}$ (000)	3538892.918	0.332	2983.3963	32.9237	2.446 (−47)	2.732 (−10)	8.941 (−04)	6.121 (−03)
$11_{4,8}-10_{5,5}$ (000)	3547271.514	0.074	1724.7054	2.9745	1.125 (−27)	2.343 (−06)	8.619 (−03)	2.052 (−02)
$6_{2,5}-6_{1,6}$ (010)	3553520.985	0.106	2042.7533	18.2870	1.210 (−32)	2.380 (−07)	4.872 (−03)	1.515 (−02)
$6_{0,6}-5_{1,5}$ (010)	3566075.414	0.075	1922.8290	16.0025	9.043 (−31)	5.652 (−07)	6.064 (−03)	1.705 (−02)
$10_{3,8}-11_{0,11}$ (000)	3568076.852	0.086	1327.1100	0.1497	1.830 (−21)	4.107 (−05)	1.771 (−02)	3.021 (−02)
$13_{4,9}-13_{3,10}$ (000)	3569620.105	0.156	2414.7234	80.0370	1.871 (−38)	1.643 (−08)	2.506 (−03)	1.065 (−02)
$6_{0,6}-5_{1,5}$ (000)	3599641.679	0.010	326.6255	16.8349	7.794 (−06)	5.518 (−02)	1.079 (−01)	7.953 (−02)
$3_{2,2}-2_{1,1}$ (010)	3601635.514	0.097	1693.6499	5.5060	3.441 (−27)	2.957 (−06)	9.239 (−03)	2.144 (−02)
$8_{3,6}-8_{2,7}$ (000)	3612970.788	0.016	885.6002	34.8092	1.445 (−14)	9.917 (−04)	3.963 (−02)	4.668 (−02)
$7_{2,5}-6_{3,4}$ (010)	3623900.400	0.125	2271.7122	13.3818	3.211 (−36)	4.640 (−08)	3.285 (−03)	1.239 (−02)
$5_{4,1}-5_{3,2}$ (010)	3638527.781	0.065	2130.4943	20.1899	5.161 (−34)	1.285 (−07)	4.250 (−03)	1.424 (−02)
$7_{3,5}-7_{2,6}$ (010)	3639916.806	0.114	2318.5399	10.9426	5.960 (−37)	3.322 (−08)	3.032 (−03)	1.189 (−02)
$6_{1,6}-5_{0,5}$ (000)	3654603.510	0.011	325.3479	50.7123	8.168 (−06)	5.622 (−02)	1.097 (−01)	8.077 (−02)
$6_{1,6}-5_{0,5}$ (010)	3657072.544	0.089	1920.7665	48.3241	9.754 (−31)	5.828 (−07)	6.226 (−03)	1.750 (−02)
$6_{1,5}-5_{2,4}$ (010)	3660797.270	0.121	2024.1526	8.0879	2.367 (−32)	2.772 (−07)	5.174 (−03)	1.586 (−02)
$8_{3,5}-7_{4,4}$ (000)	3669872.287	0.016	927.7439	3.2017	3.176 (−15)	7.395 (−04)	3.725 (−02)	4.550 (−02)
$11_{3,8}-11_{2,9}$ (000)	3674227.170	0.064	1690.6644	57.1298	3.836 (−27)	3.060 (−06)	9.456 (−03)	2.191 (−02)
$9_{2,7}-9_{1,8}$ (000)	3682708.059	0.024	1079.0796	37.0826	1.373 (−17)	2.495 (−04)	2.847 (−02)	3.948 (−02)
$7_{2,6}-7_{1,7}$ (000)	3691315.397	0.013	586.4792	6.1064	6.809 (−10)	8.645 (−03)	6.918 (−02)	6.347 (−02)
$4_{4,0}-4_{3,1}$ (010)	3708481.568	0.049	2005.9170	3.5876	4.564 (−32)	3.186 (−07)	5.409 (−03)	1.634 (−02)
$11_{5,6}-10_{6,5}$ (000)	3718095.717	0.075	1874.9730	9.5087	5.069 (−30)	8.185 (−07)	6.861 (−03)	1.857 (−02)
$8_{5,3}-8_{4,4}$ (000)	3721502.738	0.015	1131.7756	13.7798	2.065 (−18)	1.719 (−04)	2.614 (−02)	3.791 (−02)
$9_{4,6}-9_{3,7}$ (000)	3737021.502	0.022	1216.2312	15.8717	9.900 (−20)	9.387 (−05)	2.254 (−02)	3.510 (−02)
$4_{4,1}-4_{3,2}$ (010)	3740915.716	0.059	2004.8157	10.7218	4.750 (−32)	3.229 (−07)	5.462 (−03)	1.649 (−02)
$5_{4,2}-5_{3,3}$ (010)	3756027.136	0.061	2126.4077	6.6282	5.989 (−34)	1.350 (−07)	4.405 (−03)	1.473 (−02)
$13_{4,10}-12_{5,7}$ (000)	3762739.966	0.182	2300.6850	2.3461	1.135 (−36)	3.856 (−08)	3.225 (−03)	1.248 (−02)
$12_{4,9}-11_{5,6}$ (000)	3776068.455	0.118	1998.9953	8.4162	5.859 (−32)	3.386 (−07)	5.565 (−03)	1.673 (−02)
$6_{4,3}-6_{3,4}$ (010)	3797448.282	0.074	2271.7122	28.1137	3.219 (−36)	4.777 (−08)	3.425 (−03)	1.295 (−02)
$6_{1,5}-5_{2,4}$ (000)	3798281.643	0.012	416.2087	9.1300	3.116 (−07)	2.995 (−02)	9.639 (−02)	7.677 (−02)
$4_{2,3}-3_{1,2}$ (000)	3807258.625	0.013	173.3658	20.2156	1.937 (−03)	1.721 (−01)	1.495 (−01)	9.712 (−02)
$13_{6,7}-13_{5,8}$ (000)	3809788.310	0.222	2629.3345	84.1528	8.340 (−42)	3.653 (−09)	1.805 (−03)	9.215 (−03)
$15_{3,12}-16_{2,15}$ (000)	3830892.705	0.570	2952.3938	0.4183	7.491 (−47)	3.588 (−10)	1.015 (−03)	6.794 (−03)
$7_{5,3}-8_{2,6}$ (010)	3844194.052	0.149	2595.8129	0.0280	2.786 (−41)	4.675 (−09)	1.933 (−03)	9.596 (−03)
$7_{5,2}-7_{4,3}$ (000)	3855281.345	0.014	931.2371	31.6994	2.808 (−15)	7.434 (−04)	3.868 (−02)	4.750 (−02)
$8_{6,3}-9_{3,6}$ (000)	3858098.971	0.022	1282.9191	0.0412	9.006 (−21)	5.924 (−05)	2.056 (−02)	3.392 (−02)
$4_{4,1}-5_{1,4}$ (010)	3859413.515	0.129	2000.8630	0.0142	5.484 (−32)	3.386 (−07)	5.656 (−03)	1.704 (−02)
$7_{1,6}-7_{0,7}$ (010)	3869939.054	0.122	2180.6429	19.1236	8.526 (−35)	9.304 (−08)	4.103 (−03)	1.438 (−02)
$7_{4,4}-7_{3,5}$ (010)	3883916.369	0.090	2439.9544	11.8138	7.585 (−39)	1.444 (−08)	2.582 (−03)	1.125 (−02)
$9_{2,7}-9_{1,8}$ (010)	3906841.074	0.166	2688.0799	38.6372	1.009 (−42)	2.431 (−09)	1.661 (−03)	8.918 (−03)
$6_{5,1}-6_{4,2}$ (000)	3922858.086	0.014	757.7802	7.3413	1.440 (−12)	2.616 (−03)	5.367 (−02)	5.702 (−02)

TABLE 4—*Continued*

Transition	ν_{ab} (MHz)	Uncertainty ($\frac{1}{2}\ \sigma$)	E_l (cm^{-1})	$\mu^2 S$	I (50 K)	I (200 K)	I (800 K)	I (1500 K)
$12_{5,8}$–$11_{6,5}$ (000)........	3937072.760	0.127	2144.0463	11.0204	3.182 (−34)	1.223 (−07)	4.450 (−03)	1.514 (−02)
$15_{4,12}$–$16_{1,15}$ (000)......	3941628.787	0.619	2952.3866	0.1381	7.503 (−47)	3.650 (−10)	1.041 (−03)	6.979 (−03)
$5_{5,0}$–$5_{4,1}$ (000)..........	3949319.439	0.017	610.3412	11.7074	2.895 (−10)	7.588 (−03)	7.038 (−02)	6.610 (−02)
$6_{5,2}$–$6_{4,3}$ (000)	3953481.889	0.015	756.7248	21.9621	1.496 (−12)	2.649 (−03)	5.414 (−02)	5.750 (−02)
$7_{5,3}$–$7_{4,4}$ (000)..........	3954345.156	0.013	927.7439	10.4622	3.187 (−15)	7.741 (−04)	3.981 (−02)	4.881 (−02)
$5_{5,1}$–$5_{4,2}$ (000)..........	3956019.087	0.016	610.1144	3.9005	2.919 (−10)	7.608 (−03)	7.052 (−02)	6.622 (−02)
$8_{5,4}$–$8_{4,5}$ (000)..........	3970997.233	0.015	1122.7085	40.1678	2.870 (−18)	1.909 (−04)	2.814 (−02)	4.064 (−02)
$3_{2,1}$–$2_{1,2}$ (000)..........	3977046.138	0.011	79.4964	9.4637	5.681 (−02)	3.471 (−01)	1.840 (−01)	1.107 (−01)
$11_{2,9}$–$12_{1,12}$ (000).......	3981742.623	0.133	1557.8478	0.1407	4.574 (−25)	8.355 (−06)	1.290 (−02)	2.684 (−02)

of water—for which a combination of collisions and radiative processes must be considered. Indeed, the $1_{1,0}$–$1_{0,1}$ $\nu_2 = 1$ fundamental at 658 GHz is known to mase strongly in a number of regions (Menten & Young 1995), and a number of other low-lying $\nu_2 = 1$ transitions, such as the $1_{1,1}$–$0_{0,0}$ line reported here, should be bright masers through the same pumping mechanism. Even in the ground state, a more realistic assessment of the source structure leads to water transitions appearing both in emission and absorption (Zmuidzinas 1996). A detailed understanding of how water is excited, including maser action, requires knowledge of both the radiation and density environment along with the strengths of the ν_2 band transitions. The line strengths for the ν_2 band have been measured in some detail for the atmospheric community and can be found in Toth (1998). The Toth (1998) line strengths are given in centimeters squared per atmosphere at 296 K and can be converted to the nm^{2}MHz units used in the JPL catalog by multiplying by a factor of 247938.0 (Avogadro's number divided by a mole volume in centimeters cubed at 296×10^{-14} K). The factor of 10^{-14} converts the nanometers squared megahertz JPL catalog unit into centimeters squared megahertz units, which are often more natural for calculations. Division by a factor of $2.99792458 \times 10^{18}$ converts the catalog units into the commonly given infrared units per centimeter (molecule cm^{-2})$^{-1}$.

TABLE 5

THE ROTATIONAL PARTITION FUNCTION OF WATER VAPOR

Temperature (K)	Q_{rs}	Correction
9.375	1.2572	1.00000000
18.750...........	3.0332	1.00000000
37.500...........	8.5802	1.00000000
50.000...........	12.9613	1.00000000
75.000...........	23.1702	1.00000000
100.000	35.1523	1.00000000
150.000	63.6774	1.00000000
200.000	97.4129	1.00000000
225.000	116.0195	1.00000000
300.000	178.1163	1.00000031
400.000	274.5588	1.00001526
500.000	386.2616	1.00016408
800.000	818.9779	1.00640974
1000.000	1193.9312	1.02295710
1500.000	2429.2597	1.14104678

4. CONCLUSIONS

Recently, *ISO* has observed a large number of water emission lines in a wide variety of astronomical sources. As a result, the pivotal role water plays in cooling oxygen-rich molecular gas is now well established. If the high temperatures inferred from CO observations of many of these regions are proven to apply to water as well, the number of states considered in the current models are grossly inadequate, and most of the details of the excitation dynamics have been blended by a near continuum of water emission lines. At such high temperatures, very high spectral resolution is required to deconvolve the true continuum. Heterodyne observation of lines such as those presented in this paper should facilitate direct observations of hot sources and measurements of the rotational temperatures therein. An accurate temperature measurement will define the severity of the prediction problem for water. If the temperature really is much above 300 K, future missions such as *FIRST* and SOFIA will observe many strong water lines, including a large number above the energies considered here. Analyses of these observations will require extended calculations that include a good many more quantum states than those considered here, especially levels in the $\nu_2 = 2$, $\nu_1 = 1$, and $\nu_3 = 1$ states, and a great deal more laboratory work. At a minimum, the data presented here should be sufficient for planning observations of all but the most highly shocked and hottest regions.

Parts of the research described in this paper were carried out by the Jet Propulsion Laboratory, California Institute of Technology, under contract with the National Aeronautics and Space Administration (NASA). G. A. Blake acknowledges the support of NASA and the National Science Foundation. We thank Simon Verghese of MIT Lincoln Laboratories for supplying the photomixers used in this study. J. C. Pearson thanks Robert A. Toth for making available his latest water measurements prior to publication and for useful discussions concerning their analysis.

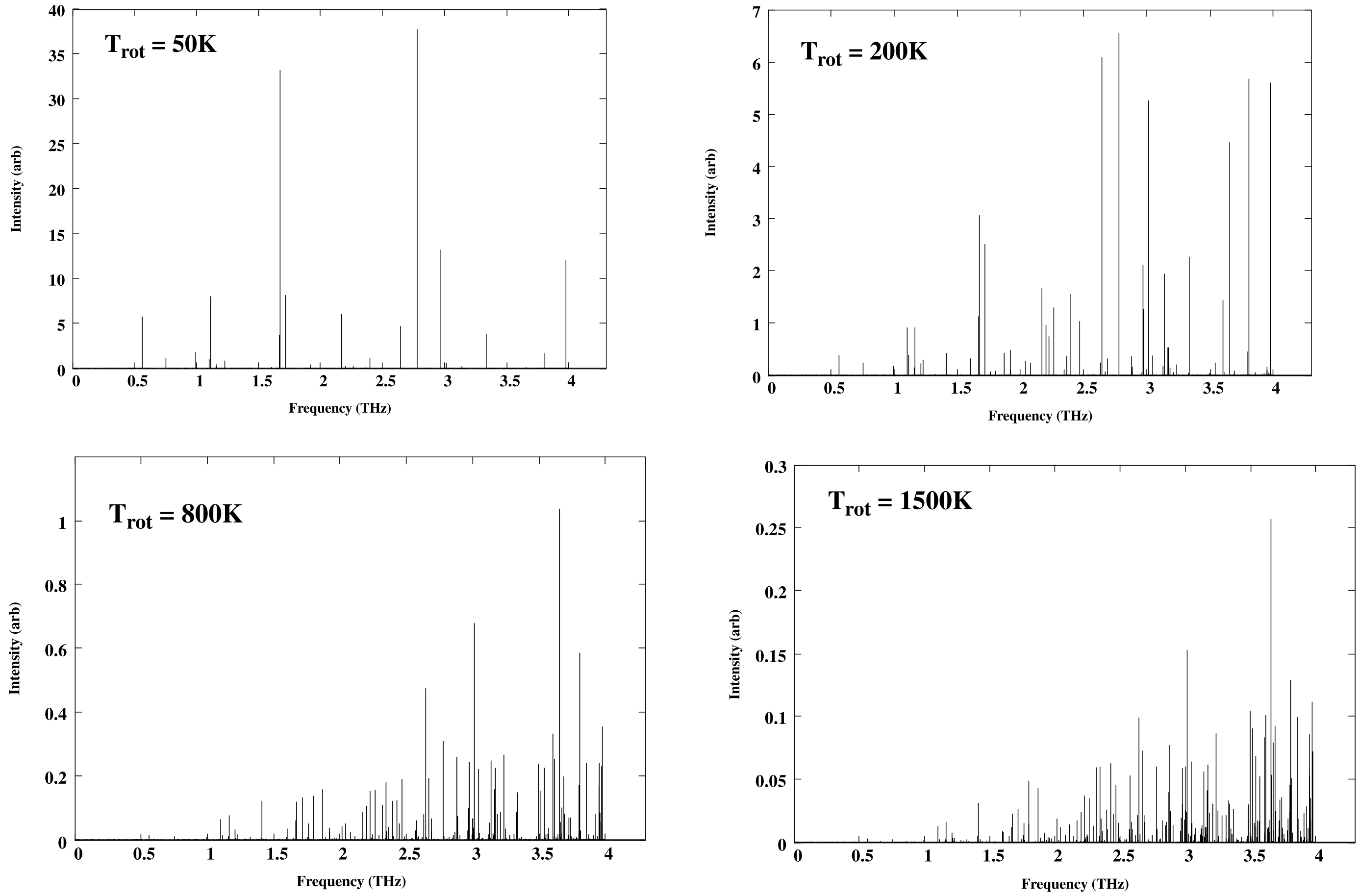

FIG. 2.—Predicted LTE spectra of water vapor from 0.5–4 THz for rotational temperatures of 50, 200, 800, and 1500 K. The column density is the same for all four plots. While the intensity is arbitrary the scaling factor is the same for all four plots, so the relative intensities are meaningful.

REFERENCES

Belov, S. P., Kozin, I. N., Polyansky, O., Yu. M., Tret'yakov, M., & Zubov, N. 1987, J. Mol. Spectrosc., 126, 113
Burenin, A., Fevral'skikh, M., Karyakin, E., Polyansky, O. L., & Shapin S. 1983, J. Mol. Spectrosc., 100, 182
Burenin, A. V., & Tyuterev, V. G. 1984, J. Mol. Spectrosc., 108, 153
Camy-Peyret, C., et al. 1985, J. Mol. Spectrosc., 113, 208
Coudert, L. H. 1992, J. Mol. Spectrosc., 154, 427
———. 1994, J. Mol. Spectrosc., 165, 406
———. 1997, J. Mol. Spectrosc., 181, 246
Csaszar, A. G., Kain, J. S., Polyansky, O. L., Zobov, N. F., &. Tennyson, J. 1998, Chem. Phys. Lett., 293, 317
Drever, R. W. P., Hall, J. L., Kowalski, F. V., Hough, J., Ford, G. M. Munley, A. J., & Ward, H. 1983, Appl. Phys. B, 31, 97
Helminger, P., Messer, J. K., & De Lucia, F. C. 1983, Appl. Phys. Lett., 42, 309
Jensen, P. 1989, J. Mol. Spectrosc., 133, 438
Johns, J. W. C. 1985, J. Opt. Soc. Am. B, 2, 1340
Kasting, J. F., Whitmore, D. P., & Reynolds, R. T. 1993, Icarus, 101, 108
Kauppinen, J., Karkkainen, T., & Kyro, E. 1978, J. Mol. Spectrosc., 71, 15
Kjaergaard, H. G., & Henry, B. J. 1994, Mol. Phys., 83, 1099
Kjaergaard, H. G., Henry, B. R., Wei, H., Lefebvre, S., Carrington, T., Jr., Mortensen, O. S., & Sage, M. L. 1994, J. Chem. Phys., 100, 6228
Lanquetin, R., Coudert, L. H., & Camy-Peyret, C. 1999, J. Mol. Spectrosc., 195, 54
Liu, X. W., et al. 1996, A&A, 315, L257
Matsuo, H., Sakamoto, A., & Matsushita, S. 1998, Proc. SPIE, 3357, 626
Matsushima, F., Odashima, H., Iwasaki, T., Tsunekawa, S., & Takagi, K. 1995, J. Mol. Struct., 352, 371
Matsuura, S., Chen, P., Blake, G. A., Pearson, J. C., & Pickett, H. M. 2000, IEEE MTT, 48, 380
Melnick, G. J. 1993, Adv. Space Res., 13, 535
Melnick, G. J., et al. 1996, Adv. Space Res., 18, 163
Mengel, M., & Jensen, P. 1995, J. Mol. Spectrosc., 169, 73
Menten, K., & Young, K. 1995, ApJ, 450, L67
Mikhailenko, S. N., Tyuterev, V. G., Keppler, K. A., Winnewisser, B. P., Winnewisser, M., Mellau, G., Klee, S., & Rao, K. N. 1997, J. Mol. Spectrosc., 184, 330
Neufeld, D. A., Chen, W., Melnick, G. J., de Graauw, T., Feuchtgruber, H., Haser, L., Lutz, D., & Harwit, M. 1996, A&A, 315, L237
Partridge, H., & Schwenke, D. W. 1997, J. Chem. Phys., 106, 4618
Paso, R., & Horneman, V. M. 1995, J. Opt. Soc. Am. B, 12, 1813
Pearson, J. C. 1995, Ph.D. thesis, Duke Univ.
Pearson, J. C., Anderson, T., Herbst, E., De Lucia, F. C., & Helminger, P. 1991, ApJ, 379, L41
Polyansky, O. L. 1985, J. Mol. Spectrosc., 112, 79
Polyansky, O. L., Zobov, N., Viti, S., Tennyson, J., Bernath, P., & Wallace, L. 1997a, Science, 277, 346
———. 1997b, J. Mol. Spectrosc., 186, 422
Pound, R. V. 1946, Rev. Sci. Instrum., 17, 490
Radford, S. J. E., & Holdaway, M. A. 1998, Proc. SPIE, 3357, 486
Shostak, S. L., Ebenstein, W. L., & Muenter, J. S. 1991, J. Chem. Phys., 94, 5875
Shostak, S. L., & Muenter, J. S. 1991, J. Chem. Phys., 94, 5883
Starikov, V. I., Taskun, S. A., & Tyutrev, V. G. 1992, J. Mol. Spectrosc., 151, 130
Suhm, M. A., & Watts, R. O. 1991, Mol. Phys., 73, 463
Tennyson, J., & Polyansky, O. L. 1998, Contemp. Phys., 39, 283
Toth, R. A. 1998, J. Mol. Spectrosc., 190, 379
———. 1999, J. Mol. Spectrosc., 194, 28
Tyuterev, V. G. 1992, J. Mol. Spectrosc., 151, 97
Verghese, S., McIntosh, K. A., & Brown, E. R. 1997, Appl. Phys. Lett., 71, 2743
Viti, S., Tennyson, J., & Polyanksy, O. L. 1997, MNRAS, 287, 79
Watson, J. K. G. 1971, J. Mol. Spectrosc., 40, 536
Zmuidzinas, J. 1996, in Proc. 30th ESLAB Symp. (ESA SP-388; Noordwijk: ESA), 151